Analysis of piles in a residual soil—The ISC'2 prediction

Fellenius, B.H., Santos J.A., Viana da Fonseca, A., 2007.
Analysis of piles in a residual soil—The ISC'2 prediction.
Canadian Geotechnical Journal 44(2) 201-220.

Analysis of piles in a residual soil—The ISC'2 prediction

Bengt H. Fellenius, Jaime A. Santos, and António Viana da Fonseca

Abstract: The 2nd International Conference on Site Characterization (ISC'2), held in 2004, included a seminar for prediction of pile capacity involving three 6 m embedment length test piles, one 350 mm square driven concrete pile, and two 600 mm diameter, strain-gage instrumented, bored piles. Invited predictors were provided with results of in situ, laboratory tests and dynamic tests. Test layout, soil information, and pile data are presented with calculations of pile capacity and load distribution, submitted predictions, and results of the static loading tests. The CPT-calculated capacities show considerable scatter—total values ranged from 500 to 1400 kN for the driven pile and from 1000 to 1900 kN for the bored piles. The static loading test on the driven pile showed an offset limit load of 1200 kN and a plunging capacity of 1500 kN. Despite pile movements of 100 mm for 1200 kN of applied load, neither of the bored piles showed signs of having reached an ultimate resistance value. Effective stress analysis of strain measurements for the bored piles showed the data to correlate to a β coefficient of 1.0 and a toe coefficient of 16. Most submitted predictions underestimated the capacity of the driven pile and overestimated the capacities of the bored piles.

Key words: pile capacity, effective stress analysis, shaft and toe resistances, β coefficient, CPTU, dynamic testing.

Résumé : Le ISC'2 tenu en 2004 incluait un séminaire sur la prédiction de la capacité des pieux impliquant trois pieux d'essai enfouis à 6 m, soit un pieu en béton de 350 mm carré foncé, et deux pieux de 600 mm de diamètre forés et instrumentés de jauges de déformation. Des participannts ont été invités à soumettre des prédictions en partant des résultats d'essais in situ et en laboratoire et d'essais dynamiques. La disposition des essais, l'information sur les sols, et les données des pieux sont présentées avec les calculs de la capacité des pieux et de la distribution de la charge, les prédictions soumises, de même que les résultats des essais de chargements statiques. Les capacités calculées sur la base du CPT montrent une dispersion considérable — les valeurs totales variaient de 500 à 1400 kN pour le pieu foncé, et de 1000 à 1900 kN pour les pieux forés. L'essai de chargement statique sur le pieu foncé a montré une charge limite de décentrement de 1200 kN et une capacité d'enfouissement de 1500 kN. En dépit de mouvements de pieu de 100 mm pour 1200 kN de charge appliquée, aucun des pieux forés n'a montré de signes d'avoir atteint une valeur de résistance ultime. L'analyse en contrainte effective des mesures de déformation pour les pieux forés a montré les données pour corréler avec un coefficient β de 1,0 et un coefficient de pointe de 16. La plupart des prédictions soumises ont sous-estimé la capacité du pieu foncé et surestimé les capacités des pieux forés.

Mots-clés : capacité des pieux, analyse en contrainte effective, résistances au fût et à la pointe, coefficient β, CPTU, essai dynamique.

[Traduit par la Rédaction]

Introduction

Pile design in foundation engineering practice includes predicting the static response of a pile to an applied load. However, only rarely is the profession able to compare the predictions with measurements of the actual response of the pile to the loading. Academia seldom makes predictions, but concentrates on theoretical evaluation of known results with some verification in laboratory model scale. As Lambe (1973) pointed out, the greatest advancement of the state of the art is achieved when comparing prediction of response with actual measured performance, provided the predictions are class A, which is a forecast of an event yet to take place. It is very satisfying for a practitioner to be able to verify a design by monitoring a full-scale response of a foundation. With regard to full-scale field tests, there is usually never time—neither in terms of hours to spend for the effort nor in terms of years to wait for the response to develop. The static loading test on a single pile being an exception and an event that allows for both to be considered. On occasions, there have been interesting and worthwhile pile foundation engineering "pile prediction seminars". More notably, T.W. Lambe's seminar at MIT in 1973 and, amongst others, the FHWA seminar in Baltimore in 1986, ASCE Foundation Engineering Congress in Evanston in 1989, and the ASCE GeoInstitute's Deep Foundation Conference in Orlando in February 2002. Participation in a prediction seminar can be

Received 13 January 2006. Accepted 31 August 2006. Published on the NRC Research Press Web site at http://cgj.nrc.ca on 17 April 2007.

B.H. Fellenius.[1] Bengt Fellenius Consultants Inc., 1905 Alexander Street SE, Calgary, AB T2G 4J3, Canada.
J.A. Santos. Instituto Superior Técnico, Technical University of Lisbon, Lisbon, Portugal.
A. Viana da Fonseca. Faculty of Engineering of the University of Porto, Porto, Portugal.

[1]Corresponding author (e-mail: bengt@fellenius.net).

 doi:10.1139/T06-105

somewhat humbling, as it invariably reveals the limits of one's knowledge, but it is also very entertaining and always educational. To quote from Lambe (1973) "Geotechnical engineering is especially damned and blessed by the importance of predictions and the difficulty of making accurate predictions."

In the fall of 2003, the Faculty of Engineering of the University of Porto (FEUP), Porto, Portugal, and the High Technical Institute (Instituto Superior Técnico) of the Technical University of Lisbon (ISTUTL), Lisbon, Portugal, invited the international geotechnical community to participate in a prediction event on pile capacity and pile load-movement response to an applied loading sequence. The event was organized by FEUP and ISTUTL in collaboration with the Portuguese Geotechnical Society, Technical Committee 18 (Deep Foundations, TC18) of the International Society for Soil Mechanics and Geotechnical Engineering (ISSMGE), and the organizers of the 2nd International Conference on Site Characterization (ISC'2) in Porto in September 2004. In December 2003, a total of 33 persons from 17 countries submitted predictions. Static loading tests were then performed. A summary of the capacity predictions and the static loading tests has been published by Santos et al. (2005). This paper presents the steps involved in preparing a prediction for the event, analysis of the relevant site and test data, and the results of the prediction efforts.

Site, soil, and pile data particulars

Test layout

The test site is a part of the ISC'2 experimental site on the campus of FEUP. In late August 2003, 12 cast-in-place piles were installed within an approximately 0.7 m deep excavation over an area of 10 m × 20 m. Two were 600 mm diameter bored piles, two were 600 mm diameter augered (CFA) piles to a 6 m depth, and eight were 600 mm diameter bored piles installed to a 22 m depth to serve as reaction piles for static testing. A few weeks later, two 350 mm square precast concrete piles were driven to a depth of 6 m. The layout of the piles in the plan is shown in Fig. 1 along with the layout of seven CPTU soundings and five boreholes.

Soil description and CPTU profile

The soil at the site is a saprolite, a weathered granite associated with a high mean annual precipitation. The weathering process involves decomposition into sand and fine-grained soil, followed by hydrolysis of feldspars, leading to formation of kaolin. The weathering has left coarse quartz grains of sand and gravel size in a matrix of clayey plagioclase, resulting in a fabric with medium to high porosity. The resulting soils are generally classified as silty sands and clayey sands. The groundwater table lies at a 10–12 m depth. Soil boring SPT N-indices indicate compact conditions. For a detailed description and results of laboratory testing, see Viana da Fonseca et al. (2004, 2006) and Santos et al. (2005), and refs. therein.

Grain-size analysis on samples from the site show about 10% clay size, 30% silt size, 40% sand size, and 20% gravel size, classifying the soil as "sand and silt with some gravel and some clay". Generally, the fines content is nonplastic or of low plasticity, with void ratios ranging from 0.6 to 0.8. An oedometer test (Fig. 2) on a sample from a 6.3 m depth indicates that the soil has a virtual preconsolidation, typical of a cemented relic structure of a young residual soil, such as this saprolite (Viana da Fonseca 2003). The virgin Janbu modulus number ranges from 15 to 30 and the reloading Janbu modulus number is about 100, corresponding to medium compressibility for a clay and high compressibility for a sand. The total density is 1800 kg/m^3, the natural water content ranges from 16.2% to 22.5%, and the degree of saturation ranges from 56% to 86%.

A CPTU profile is shown in Fig. 3 for a sounding CPT3, which was carried out before the site was excavated, and a sounding CPT5, carried out after the site was excavated and the piles installed. The recording interval was 20 mm for both soundings. The cone stress ranges from about 3 MPa near the ground surface to about 8 MPa at a depth of 8 m (depth reference is the excavation surface). The friction ratio is relatively constant and about 5%. The U2 pore-pressure measurements above an 8 m depth show negative values, i.e., suction, of about 10–20 KPa, indicating that the soil is unsaturated. The negative pore pressures are therefore more a sign of the tension in the soil owing to the capillary and surface tension than to any dilatant response to the cone displacing the soil.

CPTU-based soil classifications according to the methods proposed by Fellenius and Eslami (2000) and by Robertson (1990) are shown in Figs. 4*a* and 4*b* containing values from a 1.0 m depth to the end of sounding. To obtain a better resolution, the diagrams are plotted in linear scale as opposed to the conventional log scale. Both CPTU classifications, which are derived from calibrations in sedimentary soils, suggest that the dominant soil type at the site is silty clay to silty sand, which is a soil type slightly finer than indicated by the sieve analysis results.

The Robertson (1990) chart identifies parts of the soil as overconsolidated and cemented (area 9 in the chart), which is probably a correct characteristic for the site soil (Viana da Fonseca et al. 2006). However, the mechanical response of residual soils to loading is often quite different from sedimentary soils with similar densities and grain-size distributions. Nontextbook geomaterials always require experimental verification.

Pile details

The data used in the prediction event were provided by Santos and Viana da Fonseca (2003). The event involved three pairs of test piles to a 6 m embedment depth—two 350 mm square, driven, precast concrete piles (C piles), two 600 mm o.d. bored piles (E piles) installed using a temporary casing, and two 600 mm o.d. augered (CFA) piles (T piles).

The C piles, denoted C1 and C2, were driven on 17 September 2003 with a 40 kN drop hammer. High-strain dynamic testing was carried out on pile C2 at restrike a few hours after the end of initial driving. In January 2004, pile C1 was subjected to a static loading test.

The E piles, denoted E0 and E9, were constructed in August 2003 by first using a rotary drilling rig to install a temporary casing that was cleaned out using a 500 mm cleaning bucket. The external diameter of the cutting teeth at the bottom of the temporary casing was 620 mm. Concrete was

Fig. 1. Site plan (data from Santos et al. 2005).

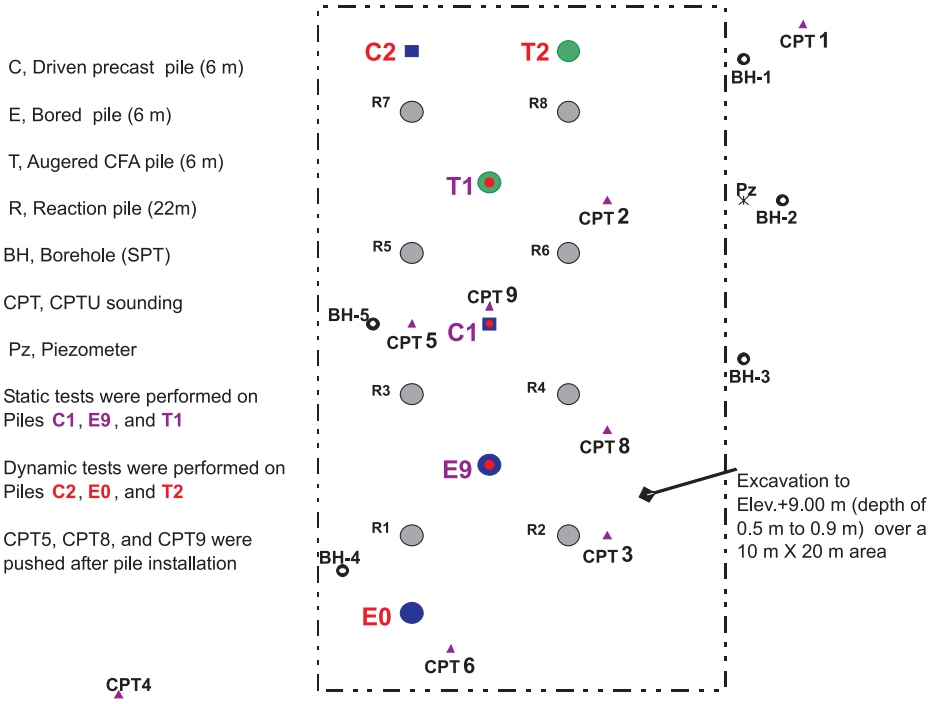

Fig. 2. Oedometer results (data from Viana da Fonseca et al. 2004).

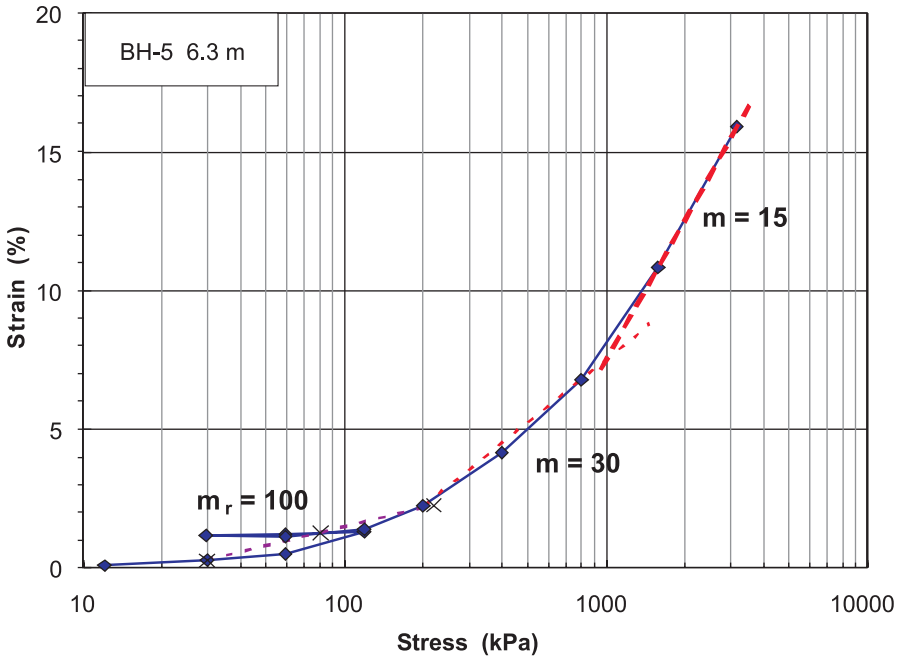

gravity placed by tremie method in the water-filled casing. Concrete slump was 180 mm and concrete "over-consumption" was below 10%. The casing was withdrawn on completion of the concreting. On 18 September 2003, high-strain dynamic testing was performed on pile E0. In January 2004, pile E9 was subjected to a static loading test.

The T piles, denoted T1 and T2, were constructed in August 2003 using a rotary drilling rig and a 600 mm continuous flight auger with a 125 mm i.d. stem. The maximum torque of the rotary head was 120 kN/m and the pull-down force was 45 kN. The auger penetration rate was approximately 25 mm/s. The concrete grout was ejected with a 6000 kPa pressure at the beginning of the grout line and a steady concrete flow of 700 L/min. Concrete slump was 190 mm and concrete overconsumption was below 6%. On 18 September 2003, high-strain dynamic testing was per-

Fig. 3. CPTU profile from CPT3 and CPT5.

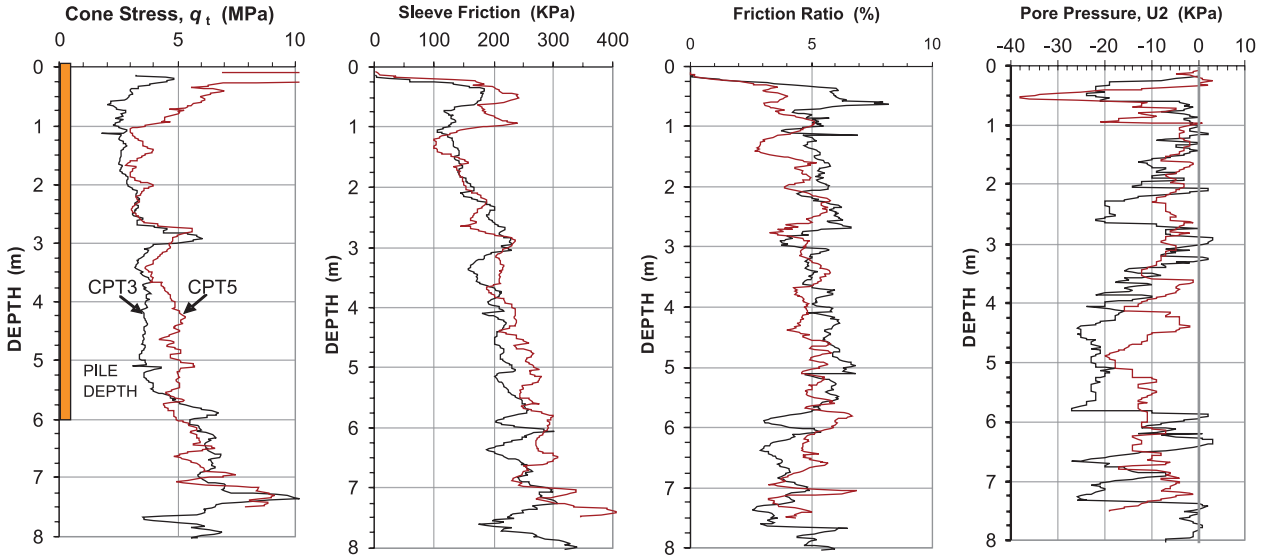

Fig. 4. (*a*) CPT3 and CPT5 plotted in Eslami–Fellenius classification chart (Fellenius and Eslami 2000). (*b*) CPT3 and CPT5 plotted in Robertson 1990 classification chart (Robertson 1990).

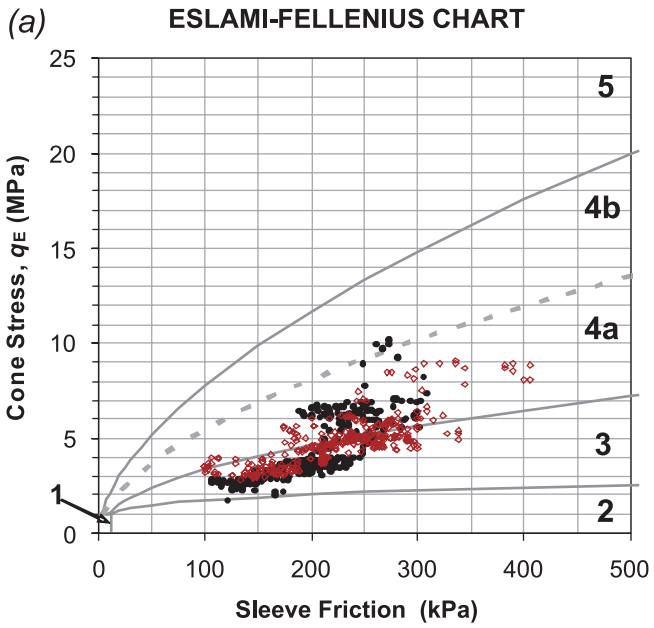

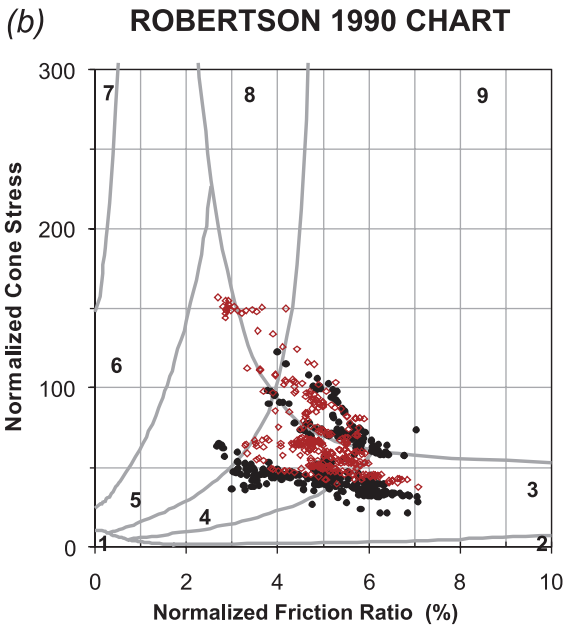

1.Very soft clays, or sensitive or collapsible soils
2.Clay and (or) Silt
3.Silty clay, stiff clay and silt
4a.Sandy silt and silt
4b.Fine sand or silty sand
5.Sand to Sandy Gravel

1.Sensitive, fine-grained soil
2.Organic soils and Peat
3.Clays [Clay to Silty Clay]
4.Silty Clay to Clayey Silt
5.Sandy Silt to Silty Sand
6.Silty Sand to Sand
7.Sand to Gravely sand
8.Sand to Clayey Sand
9.Fine-grained and overconsolidated or cemented soils

formed on pile T2. In January 2004, pile T1 was subjected to a static loading test.

Each of piles E9 and T1 was instrumented with six retrievable Geokon extensometer model A9 anchors, placed in a PVC pipe centrically cast in the pile at a 1020 mm spacing with the first anchor 150 mm below the pile head. The lowest anchor was 750 mm above the pile toe. The positions of the extensometer anchors in piles E9 and T1 are shown in Fig. 5.

The instrumentation provides the change of length (shortening) between each anchor and the lowest anchor (anchor 6) as induced by the load applied in the static loading test. A shortening between anchor points divided by the length between the points corresponds to the average strain over the distance considered.

The use of retrievable extensometer instrumentation means that the shortenings and the associated "residual" loads in the pile, which develop before the start of the static loading test, cannot be measured. Residual loads are mostly thought only to occur in driven piles. However, they can be substantial also in cast in situ piles (Fellenius 2002*a*, 2002*b*).

In addition to the anchors, a 350 mm diameter flatjack load cell was placed between two 25 mm thick, 450 mm diameter steel plates in pile E9. The load cell was connected to the bottom of the rebar cage and lowered with the cage into the pile before grouting. The operating pressure of the load cell ranged from 0 to 20 MPa. The cell pressure measured in the static loading test multiplied by the total pile cross-sectional toe area was assumed to correspond to the portion of applied load reaching the pile toe.

After the loading tests had been completed, the piles were extracted and inspected. The pile surfaces were smooth and measurements of the actual diameter of pile E9 showed it to range from 611 to 605 mm, i.e., it was marginally larger than the nominal 600 mm diameter. The measurement of the diameter at the pile toe of extracted pile E9 showed that, starting at about 0.5 m above the pile toe, the pile diameter reduced conically to a toe diameter of about 525 mm. Figure 6 shows a photo of the extracted pile and load cell.

The toe-cell pressures were converted to load by multiplication with the area of the 525 mm diameter pile toe. However, it is possible that the stress in the donut-shaped concrete zone outside the load cell experienced a stress that is different to that of the pressure inside the load cell, and, therefore, the pile toe load determined from the load-cell pressure could be under- or over-estimating the load at the pile toe to a variable and unknown degree in the test. Moreover, the pile area used in the conversion to load might be different in the beginning of the test from that toward the end.

Dynamic testing (PDA)

High-strain dynamic restrike tests were performed on piles C2, E0, and T2 on 18 September 2003, using the GRL system. Pile C2 was restruck using the same 40 kN Banut hammer used for the initial driving, while piles E0 and T2 were restruck using an 80 kN drop hammer. The test records were provided to the predictors in electronic form prior to the static loading tests.

An example of the recorded force and velocity wave traces is shown in Fig. 7. The PDA records show that for all

Fig. 5. Positions of extensometer anchors in piles E9 and T1 and the flat-jack load cell (pile E9).

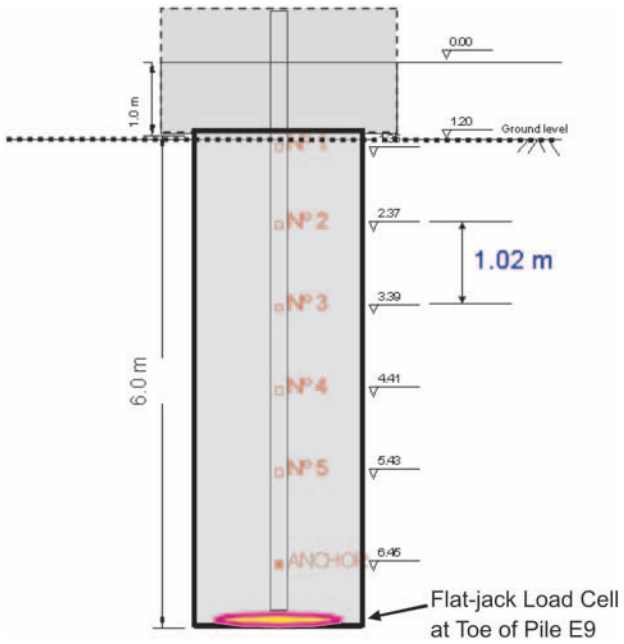

test piles significant bending occurred at the gage level during the impacts. The bending even resulted in tension values. A typical example of strains measured in a gage pair on pile C2 is shown in Fig. 8. Such reduced record quality will make the analysis of the data awkward.

Data analysis

Determining pile response to load requires a numerical treatment of pile and soil data to arrive at load distribution along the pile, load-movement response, and pile capacity. Analysis of pile response to load can be used on many kinds of data input. Everyday engineering practice differs in different countries and cultures and relies on data input from diverse in situ tests, such as the standard penetration test (SPT), pressuremeter tests (PMT), dilatometer Tests (DMT), and cone penetrometer tests (CPT and CPTU). Analysis employing input from soil parameters determined in the laboratory can consist of simple methods known as total stress (α) and effective stress (β) methods, as well as of more or less sophisticated numerical, finite element methods. Results of such analyses, be they simple or sophisticated, are unreliable for prediction of pile response, unless calibrated from results of full-scale tests. They should be thought of as methods for matching of pile response determined from other methods for the purpose of rationalizing results for application to changed conditions and for reference to other analysis results.

Of the two simple soil-input methods, the authors place the most trust in the β method because of the well-drained soil conditions. As the event is directed toward a wide audience of practicing engineers, no results of the sophisticated methods are included.

Of the four types of in situ tests SPT, DMT, PMT, and CPTU, the authors prefer to base the analysis on the CPTU

Fig. 6. Photos of the pile toe of pile E9 after extraction after the load cell had been removed from the pile (Costa Esteves 2005).

Fig. 7. Force and velocity wave traces from PDA testing on pile C2.

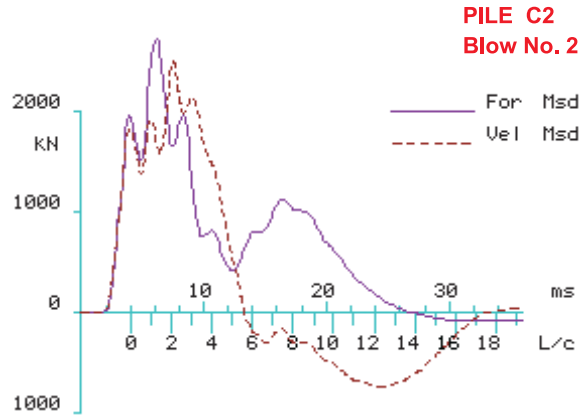

Fig. 8. Forces F1 and F2 (strain gage 1 and strain gage 2) from PDA testing of pile C2 versus time.

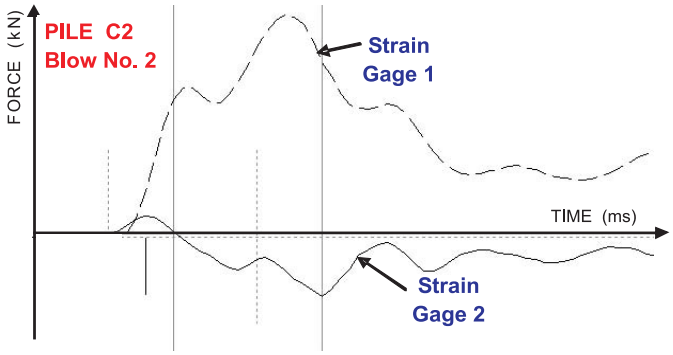

data because it is continuous and representative for the spatial variations at the site.

Dynamic tests and computer analysis of dynamic measurements to produce a response to static load are sometimes thought to be predictions. However, a dynamic test is no more a prediction than is a static loading test, as both are direct measurements of the response to load. When static and dynamic tests and subsequent analysis of the test data are executed at a sufficiently high technical level, which is an important condition, the analysis results from the two are generally close. It would seem, therefore, that the participants in the prediction event who made use of the information from the dynamic tests would have had a distinct advantage over those who did not. However, the fact that the record quality is less than desired and that the dynamic tests were made on "companion" piles and not on the piles actually subjected to static loading tests does introduce the question as to how closely the results of the CAPWAP calculations of the records from the dynamically tested piles (C2, E0, and T2) will resemble the response of the statically tested piles (C1, E9, and T1). Moreover, the necessary correction for bending influence on the gage values could cause the CAPWAP determined (simulated) capacities to become less assured.

Analysis using cone penetration soundings, CPT, and CPTU

Several methods exist for the direct calculation of pile response to load—in terms of load distribution and capacity—from CPT and CPTU soundings. The following five CPT methods and one CPTU method are in general use, depending on the country: the Dutch method (DeRuiter and Beringen 1979), the Schmertmann method (Schmertmann 1978), the LCPC method (Bustamante and Gianeselli 1982, as quoted by the Canadian Geotechnical Society (1992) in the *Canadian Foundation Engineering Manual* (CFEM)), the Meyerhof method (Meyerhof 1976; limited to piles in sand), and the Tumay method (Tumay and Fakhroo 1981; limited to piles in clay). The CPTU method is the Eslami–Fellenius method (E–F CPTU; Eslami 1996; Eslami and Fellenius 1997). A major distinction between the CPT and the CPTU methods is that CPT data do not include a correction of the cone stress, q_c, for the pore pressure, U2, acting on the cone shoulder. For the subject site, where the measured pore pres-

sures are small, the consequence of this distinction is small, however. A more significant difference in the application of the methods to the site is that, while the CPT methods require outside input of soil type and then only differentiates between two soil types, "clay" and "sand", the E–F CPTU method takes the soil denotation from the cone results. It also separates the soil denotation on six soil types as opposed to just two.

It is thought that the cone resembles a pile and, therefore, the cone penetrometer test should be able to correlate well to the load response of a pile. However, the response of the soil to a cone penetrating at a constant rate (20 mm/s) into the soil, remolding the soil and sometimes producing significant excess pore pressure, is quite different to the response to static loading of a pile. It is therefore more a surprise that empirical correlation can be produced between cone results and pile static response to load. However, the correlations must be recognized as specific to the geologic conditions and the results of the static loading tests where the correlations ("calibrations") were obtained. Therefore, different methods should be expected to produce different results in different localities, with different methods at some sites agreeing better or worse with results from static test, taking turns, so to speak, in being the "best method".

Ultimate shaft resistance is a well-defined phenomenon. However, toe resistance is a function of toe movement and does not show an ultimate value (Fellenius 1999). Moreover, toe resistance is highly dependent on the method used for defining the pile capacity from the load-movement curve of the static loading test used. The quoted CPT correlations made use of tests where different definitions of capacity were applied, all of which depend on pile length and distribution between pile shaft and toe resistances. To rationalize the approach somewhat, it is usual to correlate the cone stress toe resistance value to a toe movement representative for the toe movement incurred in a static loading test at the offset limit method (Davisson 1972; CFEM 1992), although the offset-limit value is derived from the pile *head* movement. The offset limit includes the effect of the pile length, but not the distribution between the shaft and toe resistances. At the offset limit, the pile toe movement is usually smaller than 10 mm, almost regardless of pile diameter. As most CPT correlations are made for small diameter piles, about 0.3 m in diameter, to avoid overestimating the pile toe resistance in the case of larger diameter piles, the CPT-determined value should be reduced by the inverse ratio of the pile diameter to a pile of 0.3 m in diameter (as recommended by Meyerhof (1976)).

The mentioned CPT methods have been applied to the two CPTU soundings presented in Fig. 3 employing the UniCone program (Fellenius and Infante 2002). The results are plotted in Figs. 9 and 10, as applied to pile C. Figures 9*a* and 10*a* show the distributions of unit shaft resistance and Figs. 9*b* and 10*b* show the distribution of total shaft resistance (accumulation of the unit resistance) for pile C. As the soil type straddles the border between a sandy silty clay and a clayey silty sand, the calculations are made for both sand and clay methods. The LCPC and Meyerhof methods apply slightly different shaft correlations (i.e., the ratio of shaft resistance to the uncorrected q_c) for a bored pile as opposed to a driven pile. Therefore, for the LCPC and Meyerhof methods, the calculated unit shaft resistances for piles E and T are different from that of pile C. The results for the E–F CPTU method have been calculated applying an average correlation coefficient of 0.020 to avoid exhibiting extra scatter of the curves by using the originally recommended coefficients of 0.025 and 0.015 depending on whether the data points plot above or below the line (the line between areas 3 and 4a) separating the soil type in the classification chart (Fig. 4).

The pile total shaft and toe resistances and total capacities resulting from the application of the CPT methods and the E–F CPTU method for CPT3 and CPT5 to pile C are compiled in Table 1.

The most noticeable result of the calculations is that they show a large spread from a total shaft resistance of about 100 kN for the Dutch method in sand through about 800 kN for the Schmertmann method in sand and a spread of toe resistance ranging from 300 kN for the Dutch method in clay through 630 kN for the Eslami–Fellenius method. The range of calculated total pile capacities is 530 through 1450 kN.

The calculated resistance distributions are plotted in Fig. 11*a* for pile C and Fig. 11*b* for piles E and T employing the "before" cone test data (CPT3). Obviously, unless the person charged with predicting the capacity has experience from the site and from prior application of the cone methods to the site soils and (or) a strong preference for one method over the others, a prediction from the cone data will be little more than a "best guesstimate".

Analysis using effective stress—Shaft resistance

Wherever a body slides against another body, small or large, the ultimate shear resistance is proportional to the effective normal stress acting between the bodies. The condition of a pile sliding against soil is no different, and the ultimate pile shaft resistance is the product of a "friction coefficient" times the normal effective stress acting against the pile shaft. The normal effective stress against the pile shaft is normally related to the overburden (vertical) effective stress via a stress ratio, K_s. While neither the normal (for vertical piles, the horizontal) stress nor the friction coefficient are simple to determine, calculation of the effective overburden stress is straightforward and does not involve much else than knowledge of soil densities and pore-pressure distribution. Usually, the intermediate factors (friction angle, coefficient of earth pressure, texture of the pile surface, rotation of stresses, effect owing to different displacements of piles of different diameter, etc.) are ignored and the shaft resistance is determined from the effective overburden stress directly by means of a proportionality coefficient called a β coefficient, which incorporates the mentioned intermediate factors.

Determining what the β coefficient governs in a specific case is not an easy matter. The CFEM (1992) recommends a β of 0.25–0.30 for clay and a β of 0.30–0.90 for sand. However, these ranges are derived from experience with sedimentary, mostly fluvially deposited soils and may not apply to residual soils. Perhaps more important, the CFEM ranges are derived from piles usually much longer than 6 m, for which the shallow-depth influence of apparent overconsolidation (explained by principles of steady-state soil mechanics) is small. Therefore, it would be expected that the β coefficient

Fig. 9. Shaft resistances for pile C determined from CPT3. (*a*) Unit shaft resistance. (*b*) Total shaft resistance.

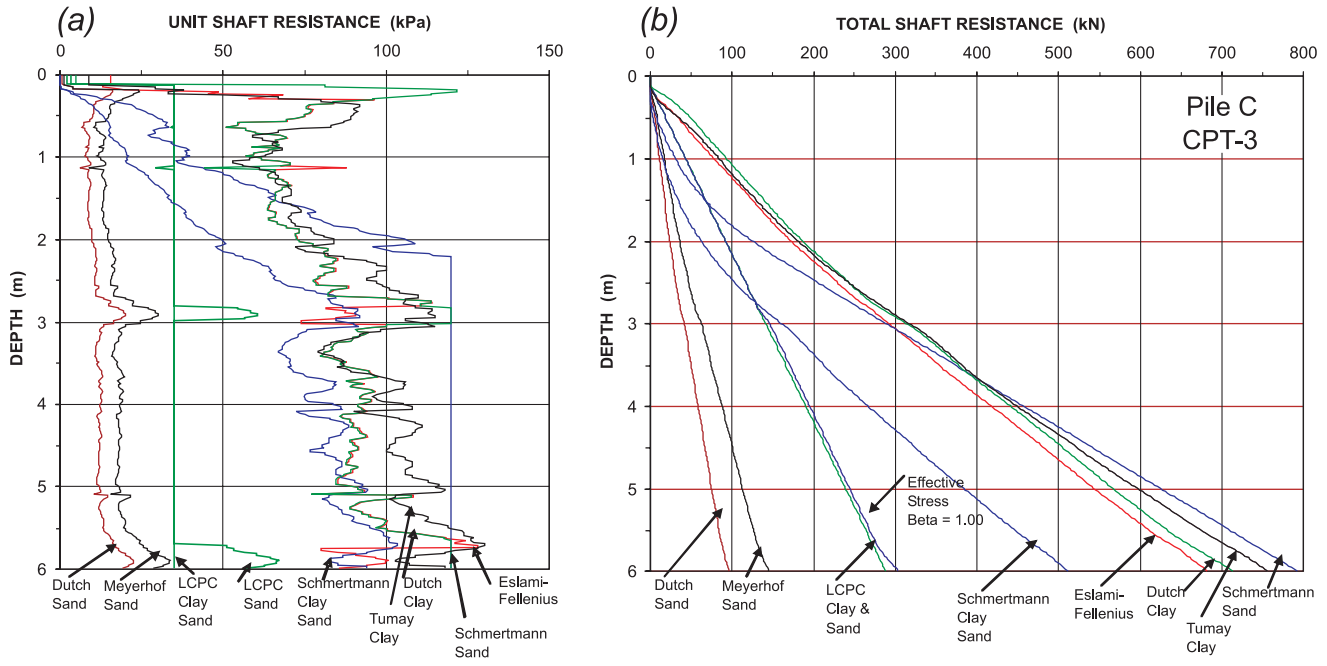

Fig. 10. Shaft resistances for pile C determined from CPT5. (*a*) Unit shaft resistance. (*b*) Total shaft resistance.

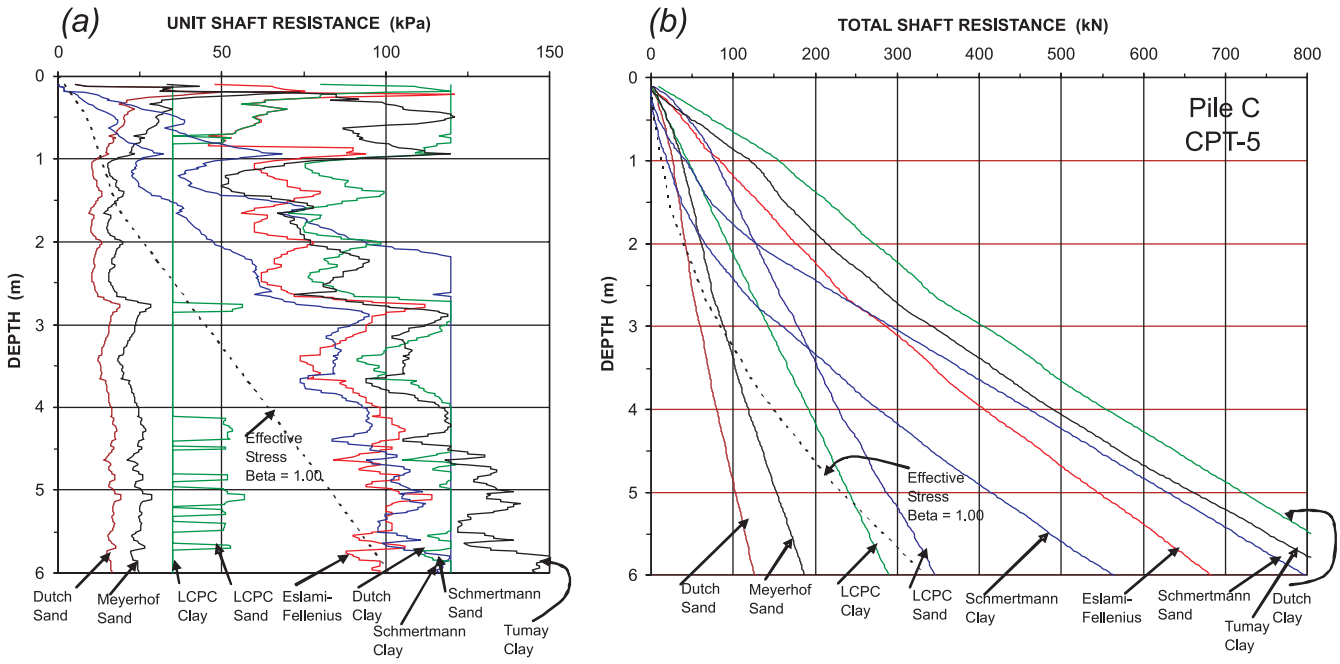

would be larger near the ground surface rather than at a deeper depth (Fellenius and Atlaee 1995). Of course, in the case of a driven pile, one must consider that the driving may have created an annulus between the pile and the soil near the ground surface.

The Hong Kong Geotechnical Engineering Office (2005) includes the following recommended β coefficients for piles in saprolite soils: driven piles, $0.1 < \beta < 0.4$, and bored piles, $0.1 < \beta < 0.6$.

Rollins at al. (2005) presented measurements of shaft resistance on a large number of piles determined in uplift static loading tests in sedimentary soils in Utah. Figure 12 presents back-calculated β coefficients for these piles. Although the data points are very scattered and the trend is diffuse, the compilation suggests that the β coefficient is largest near the ground surface and reduces with depth. For piles of 6 m length, as in this case, the β coefficient can be significantly larger than the values determined from tests on long piles.

Analysis using effective stress—Toe resistance

Deciding on what toe resistance to use involves even larger uncertainties than determining shaft resistance, primarily because an ultimate toe resistance does not truly exist. Toe re-

Table 1. Results of calculations using the CPT and CPTU methods for pile C.

	Before installation of piles (CPT3)			After installation of piles (CPT5)			
Method	Shaft (kN)	Toe (kN)	Total (kN)	Shaft (kN)	Toe (kN)	Total (kN)	% Increase of total
Eslami–Fellenius	680	565	1245	805	630	1435	16
Dutch, sand	100	430	530	125	400	525	–1
Dutch, clay	710	300	1100	880	290	1170	16
LCPC, sand	305	350	650	345	320	665	2
LCPC, clay	290	380	670	290	355	645	–4
Schmertmann, sand	790	580	1370	800	600	1400	2
Schmertmann, clay	510	580	1090	565	600	1165	7
Meyerhof	145	565	710	190	615	805	13
Tumay	540	580	1120	850	600	1450	29

Fig. 11. Distribution of resistances determined by the CPT and CPTU methods for CPT3 as applied to the test piles. (*a*) Pile C; (*b*) piles E and T.

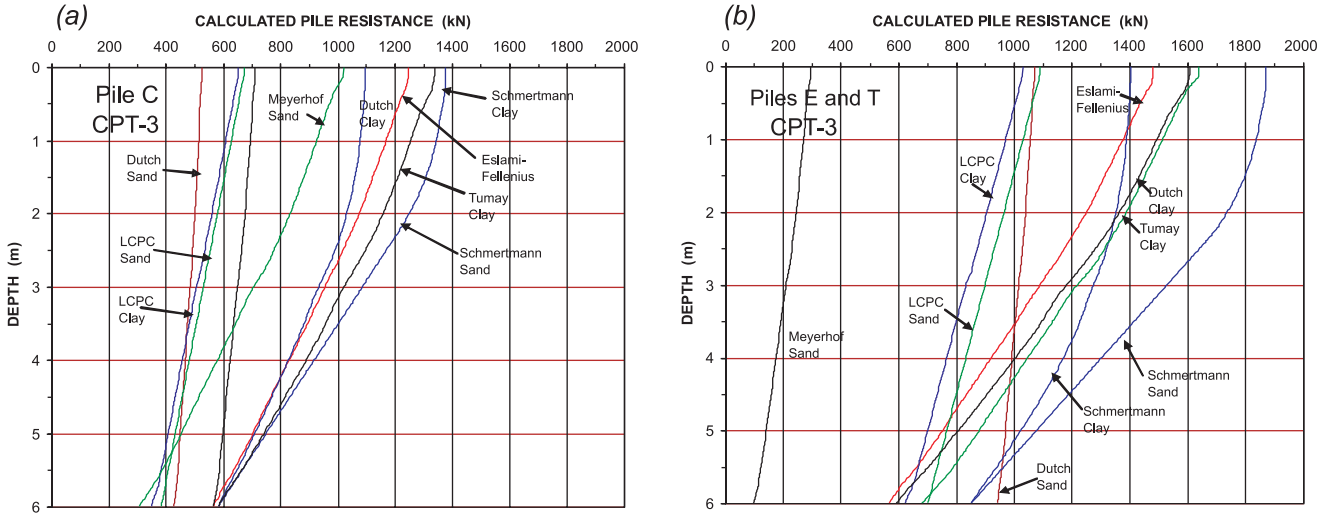

Fig. 12. β coefficients obtained from back-analysis of tension tests on bored piles in sand (data from Rollins et al. 2005) and range of values indicated for sands by the *Canadian Foundation Engineering Manual* (CFEM 1992) and for saprolites by the Hong Kong Geotechnical Engineering Office (HKGEO 2005).

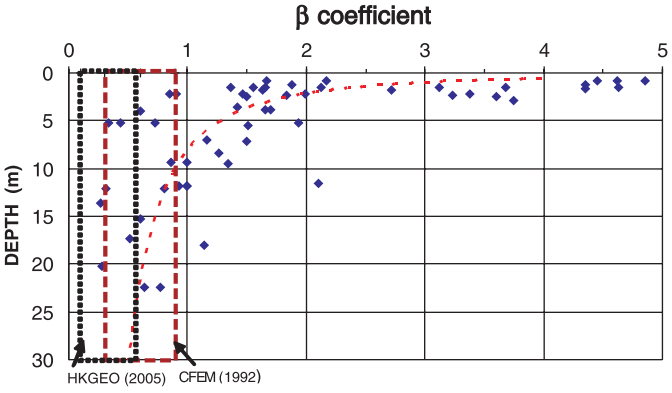

sistance is a function of toe movement and follows a more or less gently curving path that has no definite peak (Fellenius 1999). The pile-head load-movement curve from a static loading test on a pile may yet show a distinct peak value that can be taken as the capacity of the pile. However, the peak value may be due to that (*i*) minimal toe resistance is present, (*ii*) the pile increment shortening owing to adding a load increment increases once all of the ultimate shaft resistance has been mobilized, (*iii*) the shaft resistance has a postpeak softening response, and (or) (*iv*) the presence of locked-in toe load (residual load). For an applied load smaller than locked-in toe load, the pile toe moves very little, while, once reached, it moves significantly for little further increase in the toe load. The total capacity consisting of shaft and toe resistance is therefore a somewhat blurred concept. Engineering practice has resolved the conundrum by establishing definitions for capacity, e.g., the offset limit load (Davisson 1972, quoted by Fellenius 1975, 2002*b*) or the amount of load on the pile that causes a movement of 10% of the pile-head diameter measured at the pile head (European Committee for Standardization 2004), which is that the movement limit includes the pile shortening for the applied load. In a conventional static loading test, the pile toe movement induced when the offset limit load definition is satisfied is approximately 5–10 mm. Moreover, in a conventional static loading test on piles of diameters ranging from 0.3 to 0.9 m, the pile head is rarely moved beyond 40 mm. When considering shortening for the load, therefore, in other than rather short piles, the induced pile toe movement is rarely larger than 10 mm. Therefore, pile toe capac-

Table 2. PDA measurements.

Pile	Blow No.	Height of fall (m)	Pile net penetration for the blow (mean of several blows), actual mm/blow	Penetration resistance (equivalent no. of blows for a 25 mm penetration)	Maximum force in the pile (kN)	Maximum transferred energy (kJ)
C2	1	0.8	6	4	1676	7.5
	2	0.8	6	4	2754	22.4
	3	0.8	6	4	2904	24.7
E0	1	0.6	10	<1	3548	31.4
	2	0.8	20	<1	4523	47.8
	3	1.2	40	1.6	6219	71.6
	4	1.4	40	1.6	7537	90.6
T2	1	0.4	3	8	*1962*	*13.1*
	2	0.6	6	4	2987	20.3
	3	1.0	15	<1	5151	44.7
	4	1.3	20	<1	5836	57.4

Note: Values in italic font are considered poor data.

ity should be thought of as being defined as the pile toe load mobilized for a 5–10 mm magnitude of induced toe movement. Defining the load at that movement as the "toe capacity", however, does not make it into an ultimate value, nor does it mean that an ultimate value indeed exists.

Similarly to the shaft resistance, the unit toe resistance corresponding to the so-defined pile toe capacity is considered to be proportional to the effective overburden stress at the pile toe through a toe coefficient, N_t. For piles in silt, the CFEM (1992) recommends N_t values of 20–40 for driven piles and 10–30 for bored piles. For piles in sand, the CFEM recommends N_t values of 30–120 and 20–60 for driven and bored piles, respectively. These ranges are very wide.

Distributions of resistance were calculated employing the UniPile program (Fellenius and Goudreault 1998). The toe resistance coefficients, N_t, determined from the CPT methods applied to CPT3 and presented in Table 1 correlate to a range of 30–50 for piles in sand and to a range of 20–40 for piles in clay. The E–F CPTU method toe resistance corresponds to $N_t = 40$. For piles E and T, the E–F CPTU method toe resistance corresponds to $N_t = 20$.

Applying effective stress analysis, i.e., the β method, to predict the pile capacity of the test piles at the site would result in a wide range of values considering the wide range of recommended values. Again, for predicted values to be close to the forthcoming tests would require access to coefficients back-calculated from previous tests in similar soils.

Analysis using dynamic measurements

The dynamic measurements and analysis of the data gave the values presented in Table 2. The table also includes the results of the CAPWAP analyses produced before the start of the static loading tests (Fellenius and Salem 2003).

Dynamic analysis for capacity (CAPWAP) should ideally be made for penetration resistances of a few blows through about a dozen blows per 25 mm penetration. The actual pile penetrations per blow correspond to equivalent penetration resistances of about 4 blows / 25 mm for pile C2 and 8 blows / 25 mm and 4 blows / 25 mm for the first two blows on pile T2, whose values lie within the ideal range. However, the blows on pile E0 and the second two blows on pile T2 lie below the ideal range. For piles C2 and T2, the first blow record was not suitable for analysis. The CAPWAP analyses carried out for the records of the first useable blow indicated total capacities of 1380, 1465, and 1180 kN for piles C2, E0, and T2, respectively.

For pile E0, CAPWAP analysis was carried out on the records of first three blows, and for pile T0 the analysis was carried out on the second and third blows. The CAPWAP results show that the shaft resistance was about the same for the blows, but each blow mobilized a larger toe resistance.

The results of CAPWAP simulated static loading tests are presented in Fig. 13. The results indicate that the computed total capacities, as well as the shaft and toe resistances, are about equal in magnitude for all the three piles.

Prediction

Considering the range of calculated soil responses from the analytical methods and the questions about the quality of the particular dynamic measurements, had the case been a design project, where the consequence of being wrong could negatively impact a client and a building, then, short of applying an economically unsuitable factor of safety, the professional foundation recommendations at this stage would be to calibrate the site and analysis methods to a static loading test. However, as no professional project is contemplated and the only negative impact of being wrong is totally with regard to one's pride and self-esteem, a prediction, based on the available information, for the response of the three piles to applied load can be submitted free of hesitation.

The predictors were requested to provide one specific capacity value for each of the three loading tests on piles C2, E9, and T0. Thirty-three predictions were submitted of which the first author submitted one together with Mr. H. Salem (Fellenius and Salem 2003), predicting that pile C1 would show a capacity of 1200 kN and that piles E9 and T0 would both show a capacity of 1600 kN, as defined from the movement criteria. The submitted load-movement curves are presented in Fig. 14. The circled dot on the curves represents the mentioned submitted capacity values.

Energy ratio, transferred/ nominal (%)	Damping factor for CASE method estimate, RMX method matching CAPWAP	Mean shaft quake, q_s (mm)	Toe quake, q_t (mm)	CAPWAP Minimum toe displacement (mm)	CAPWAP Total (kN)	CAPWAP Shaft (kN)	CAPWAP Toe (kN)
23							
70	0.3	3.5	12	13	1,382	729	653
77							
65	0.9	1.0	17	19	1,465	847	618
75	0.2	0.5	26	28	1,494	844	650
75	0.4	0.5	35	41	1,550	846	704
81							
15							
42	0.3	0.5	13	14	1,182	549	633
56	0.3	0.6	22	25	1,457	502	954
55							

Fig. 13. CAPWAP load-movement simulations. (*a*) Pile C2; (*b*) pile E2; and (*c*) pile T2.

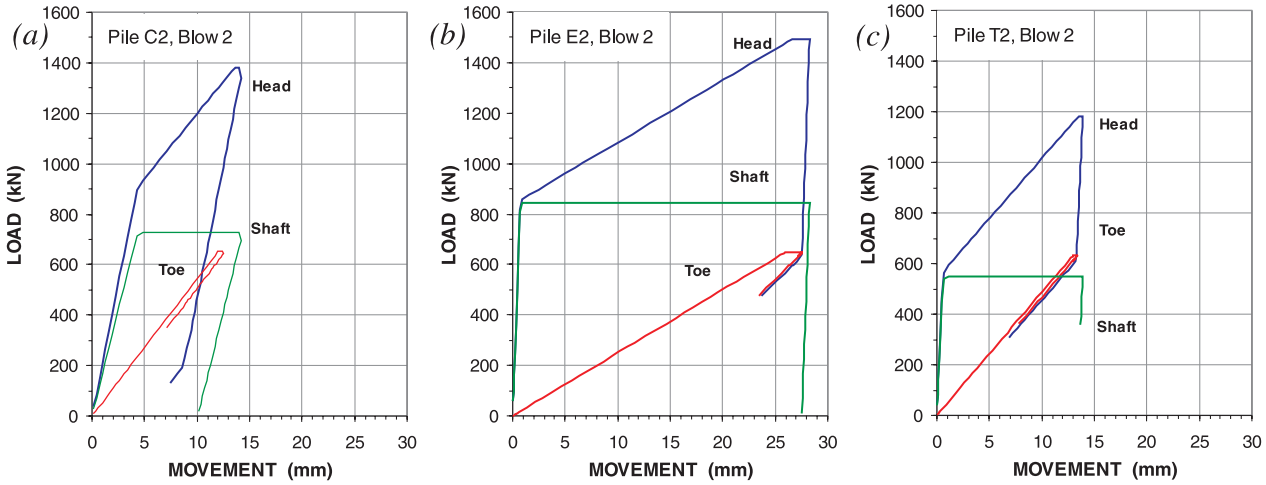

The first author's submitted prediction was based on integrating the available information into an effective stress calculation to calculate the load distribution for the piles and combining this with *t*–*z* and *q*–*z* relations for the pile shaft and pile toe to arrive at load-movement curves. In most soils, the shaft resistance reaches a peak at or before relative movement of about a "tenth of an inch", whereafter it is usually about constant (i.e., plastic response) or decreases, i.e., "strain-softening" response. In loose to compact sand, a strain hardening can occur. Accordingly, the prediction assumed a peak shaft resistance to be mobilized at a 3 mm pile toe movement with a following small postpeak strain-softening trend.

The *t*–*z* and *q*–*z* curves are based on the following expression (Fellenius 2002*a*, 2006). The expression is valid for any two points on the resistance-movement curve.

$$\frac{R_1}{R_2} = \left(\frac{\delta_1}{\delta_2}\right)^e$$

where

R_1 is the mobilized resistance;

R_2 is the ultimate resistance;

δ_1 is the movement mobilized at R_1;

δ_2 is the movement mobilized at R_2; and

e is an exponent usually ranging from a small value through unity.

A *t*–*z* shaft resistance exponent of 0.25, an average value, was applied to all three test piles. For the *q*–*z* curves, the exponents chosen for pile C1 and piles E9 and T1 were 0.4 and 0.6, respectively. The exponents were chosen from the center of the usual ranges with a smaller exponent assigned to the driven pile, pile C1, to give a stiffer toe response as opposed to the two bored piles, piles E9 and T1.

Static test results

Pile C1 was loaded in increments of 130 kN with two early unloading cycles. The offset limit was reached at an applied load of 1200 kN. When a total load of 1300 kN was reached at a pile head movement of 4.9 mm, the pile movement increased progressively. A maximum load of 1500 kN was reached at a total movement of 50 mm, after which the movement continued for a slightly decreasing load. Figures 15 and

Fig. 14. Predicted load-movement curves as submitted. (*a*) Pile C1; (*b*) piles E9 and T1.

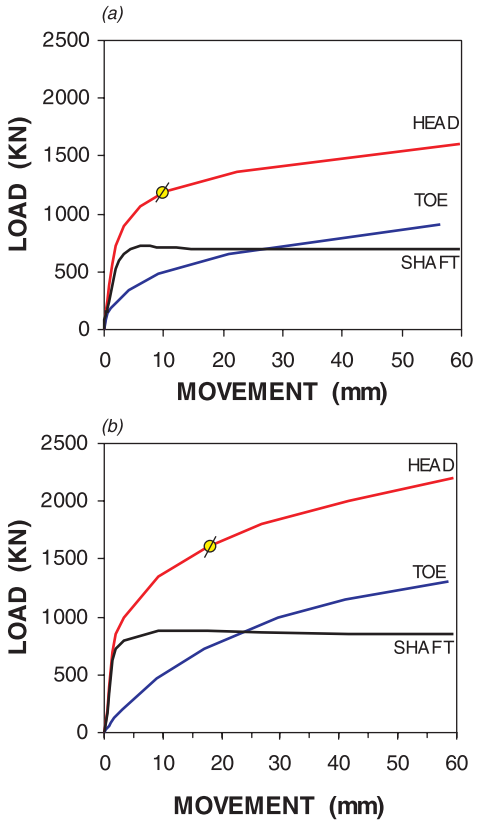

Fig. 15. Pile-head load-movements for the static loading test on pile C1 with predicted curves.

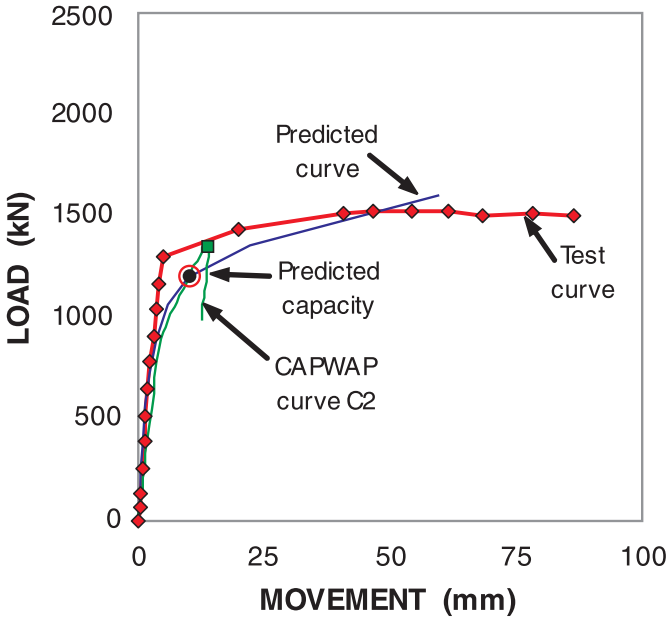

16 show the measured pile-head load-movement curves for piles C1 and E9 and T1, respectively.

Piles E9 and T1 were loaded in increments of 150 kN with two early unloading cycles. The loading sequence was

Fig. 16. Pile-head load-movements for the static loading tests on piles E9 and T1 with predicted curves. (*a*) Pile E9; (*b*) pile T1.

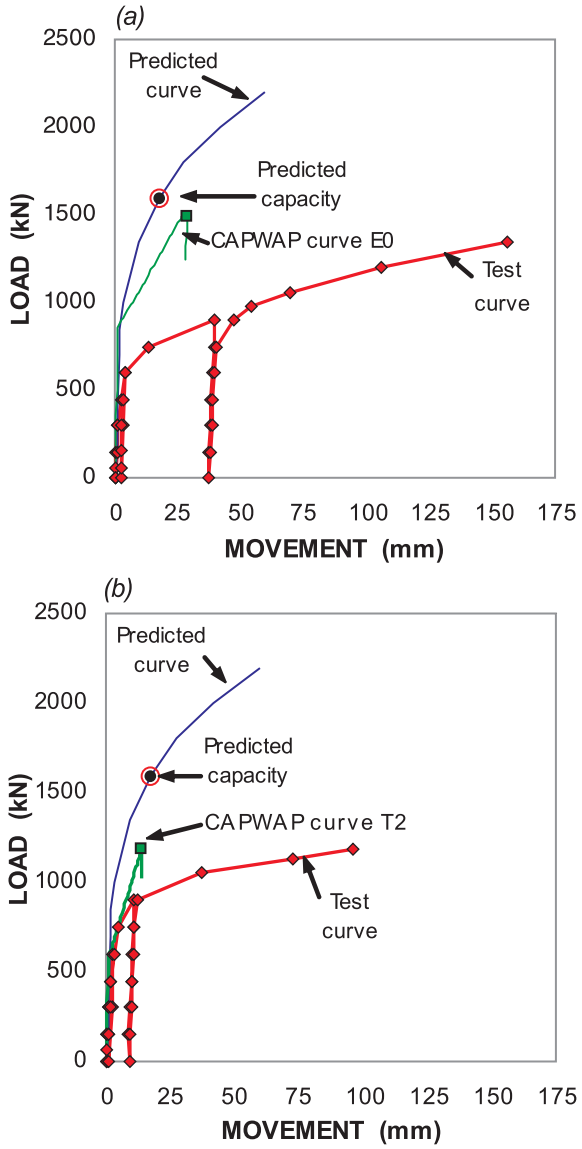

in cycles to 300 kN, followed by unloading to 600 kN, followed by unloading, and then to 900 kN followed by unloading, whereafter the piles were loaded to maximum loads of 1350 and 1200 kN, respectively. For both piles E9 and T1, the movement at 1200 kN applied load was 100 mm, i.e., 17% of the pile-head diameter.

Only the results from pile C1 exhibit a clear ultimate resistance (capacity) value. While a capacity value can be established for the curves from piles E9 and T1, for example, by the offset limit definition, no obvious load is evident that can be subjectively accepted as the pile capacity.

The prediction curves submitted by the first author and the CAPWAP simulated load-movement curves are also shown in the load-movement diagrams (Figs. 15 and 16). As can be seen, the prediction curve for the driven test pile C1 is quite good. However, both the prediction and the CAPWAP-simulated curves for piles E9 and T1 differ from the load-movement curves measured for the piles. A closer

look at the results from the extensometer measurements will indicate where the source of the difference could lie.

The five extensometers function as telltales for measuring shortening. The shortenings over the 1020 mm distance between gage points are plotted in Fig. 17. The immediate, almost glaring, measurement result is that the shortenings for pile E9 are about twice as large as those for the equivalent gage locations in pile T1. The slopes of the shortening curves (kN/mm) are proportional to the axial stiffness, EA, of the pile. The slopes corresponding to modulus values of 20 GPa in pile E9 and 40 GPa in pile T1 are indicated under the assumption that the pile diameter is equal to the nominal 600 mm value. However, to bring the slopes of the loads versus shortening curves to correspond to a 30 GPa modulus would require an 100 mm excess diameter for pile T1 and a reduction by the same amount in pile E9, i.e., to 700 and 500 mm, respectively. As mentioned above, the extracted piles showed no such diameter variation, but exhibited a smooth surface with a diameter close to the nominal one for almost the full length. Moreover, the dynamic wave speed measurements showed that all three companion piles had a dynamic modulus of close to 40 GPa. Had either of piles E0 or T2 been made of inferior concrete, it would have showed up in the dynamic test. If the difference in elastic modulus values is true, hypothetically, it could be attributed to the difference in construction methods: piles T1 and T2 by high-pressure extrusion of the grout, as opposed to piles E0 and E9 where gravity-tremie was used. The construction methods could not possibly account for a 20 GPa difference, however. The more plausible explanation is that the conversion of the readout values to actual shortening included a factor of 2 for the error. However, as discussed in the following, because the modulus used for the evaluation of shortening (strains) to load was derived from the actual relation between applied load and shortening values, rather than by an assumed typical modulus value, the evaluation of the test results is independent of whether or not the measurements include a conversion error or if the actual modulus number is true.

Converting measurements of strain to load is frequently thought to require knowledge of the dimension of the pile cross section and the Young's modulus or, rather, prior knowledge of the pile axial stiffness. However, the evaluation neither depends on knowledge of the pile diameter nor does it require separate determination of the modulus. A direct evaluation of the pile EA value can be performed by means of the tangent modulus, E_t, approach (Fellenius 1989, 2001*b*). Figure 18 shows a plot of change of stress over change of strain, E_t, for each increment of load versus total strain. (The calculations presume that the pile diameter is 600 mm over each gage length). The five thin lines show the values calculated for each 1.02 m extensometer length, and the heavy line with dots shows the sum of values over the full 5.10 m extensometer length. Such plots initially exhibit initially large E_t values that gradually reduce until the shaft resistance (at the gage location) has become mobilized, whereafter the plot continues along a more or less straight line — provided the soil does not exhibit strain softening or strain hardening and the records have good accuracy. For a steel pile, which has a constant Young's modulus, the line becomes horizontal. As the modulus of concrete is strain-dependent and reduces to a larger or lesser degree with increasing strain, lines for concrete piles are sloping. As shown by Fellenius (1989, 2001*b*), an expression for the secant modulus, E_s, or secant stiffness, E_sA, which is a function of the imposed strain, can easily be evaluated from the line and be used in determining the load for each strain value at each gage.

Fig. 17. Applied load versus pile shortening betweeen extensometer points (1020 mm apart). For the initial cycles, only the final shortenings are shown. (*a*) Pile E9; (*b*) pile T1.

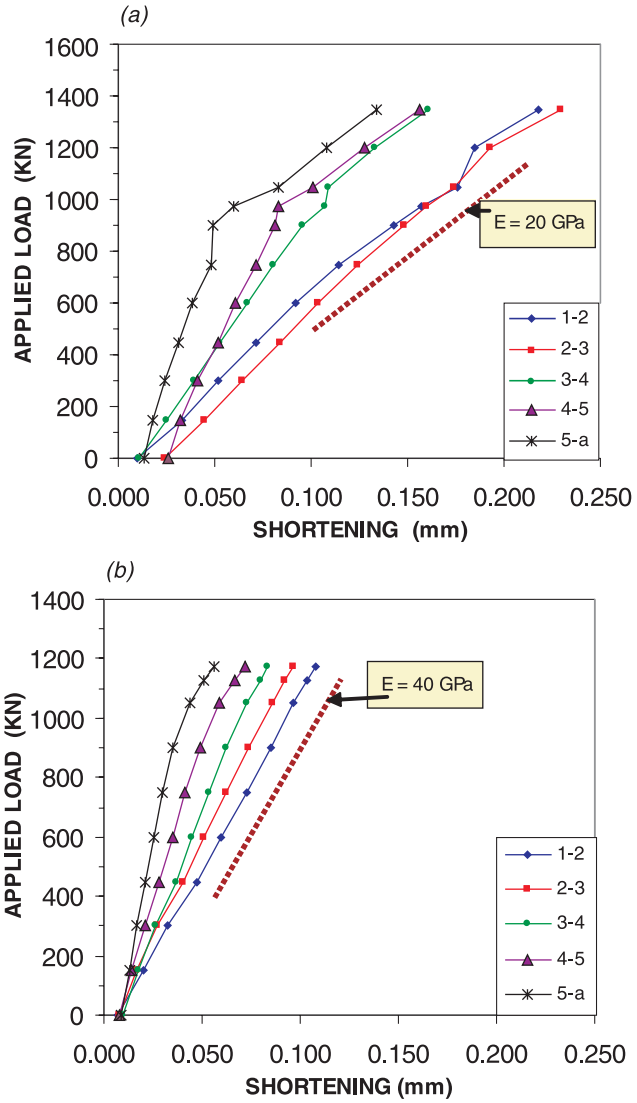

An approximate tangent-modulus straight line (the dashed lines) has been evaluated and added to each diagram. However, as indicated by the scatter shown in Fig. 18, the accuracy of the evaluation is too low to grant confidence in using this line for the secant modulus relation, in particular for pile E9. Instead, the data are evaluated by correlating the three upper extensometer values to the applied load in determining the relation between measured shortening and load. The correlations indicate Young's modulus values of 20 and 39 GPa for pile E9 and T1, respectively, based on the 600 mm nominal diameter.

Fig. 18. Tangent modulus diagram for the five gage lengths. (*a*) Pile E9; (*b*) pile T1.

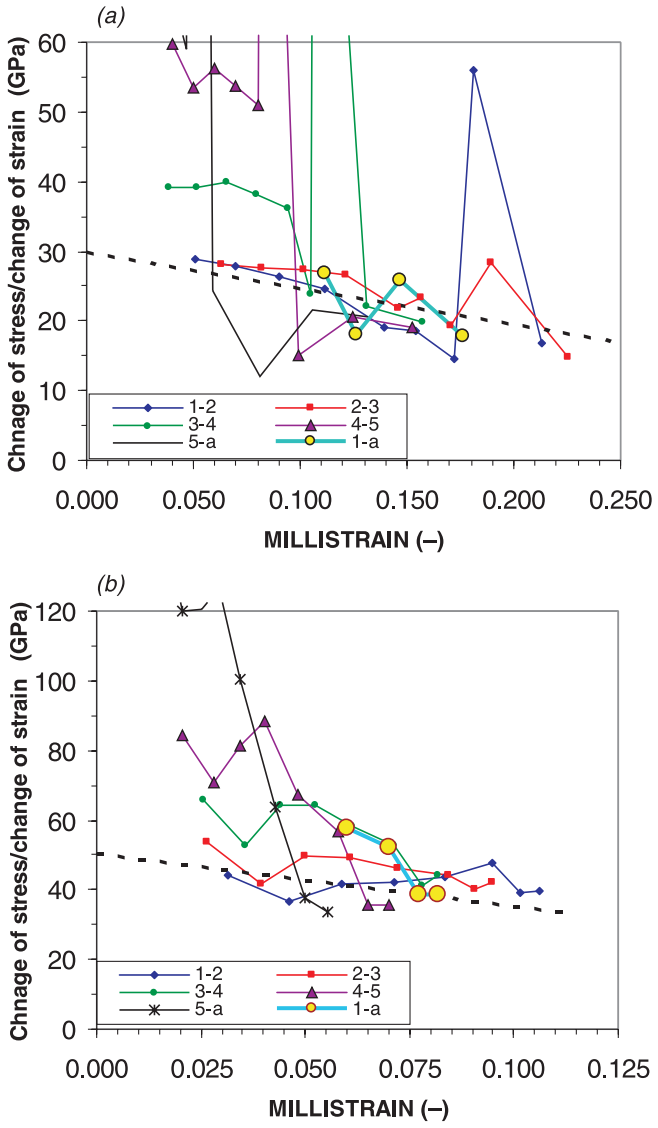

Fig. 19. Distribution of load over extensometer lengths. (*a*) Pile E9; (*b*) pile T1.

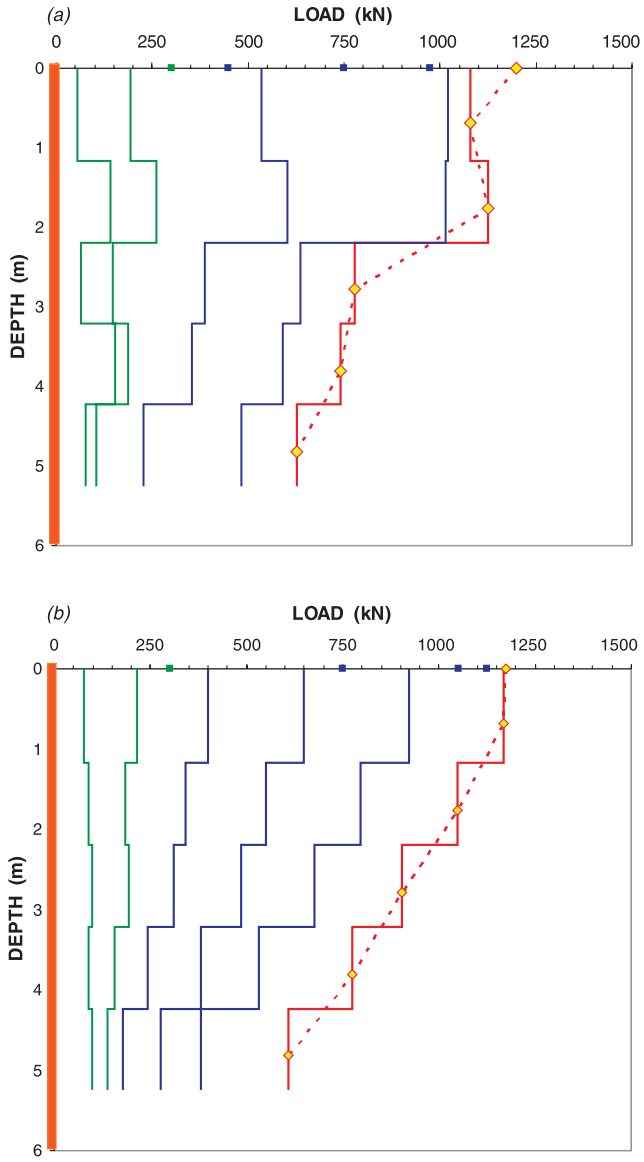

The load values calculated from the measured shortenings have been plotted in block diagrams in Fig. 19 for selected loads applied to the pile head during the last loading cycle. Each block represents the average load in the pile for the extensometer length. Assuming increasing unit shaft resistance with depth for each block, the representative average value is located at a height below the top of the extensometer length of 0.58 times the length (Fellenius 2001*a*). These average values are connected with a line for the last load representing the load distribution evaluated from the measurements.

In Fig. 20, all the determined load distributions are presented for the two instrumented test piles, E9 and T1, unloading records excluded. The curves indicating the maximum load at each pile head are from a pile-head movement of 100 mm, chosen to ensure that both piles are evaluated at the same pile head movement. Also shown for each pile is a curve for a calculation of the distribution at the maximum load fitted to an effective stress analysis. The fitted curves are calculated using a β coefficient of 1.7 at the bottom of the excavation decreasing to a value of 1.0 at the pile toe, and a toe bearing coefficient of 12. The soil density is 1800 kg/m^3. The effect of the unloading of the soil from the excavation is calculated using a 2:1 distribution.

For pile E9, most of the difference between the measured and the calculated values can be considered because of the inconsistency in the shortening values. For pile T1, where the records are sufficiently consistent to allow the trend to be allocated to small locked-in load (presence of residual load) in the pile before the start of the test. The usual assumption when analyzing residual load distribution (Fellenius 2002*a*) is to assume fully mobilized negative skin friction from the surface and down and fully mobilized positive shaft resistance from the pile toe and up, with a transition zone of some length in between. Fitting to the measured loads and using a reasonably smooth distribution of β coefficients will then provide a distribution of residual load and

Fig. 20. Load distributions: measured and fitted to effective stress analysis. (*a*) Pile E9; (*b*) pile T1.

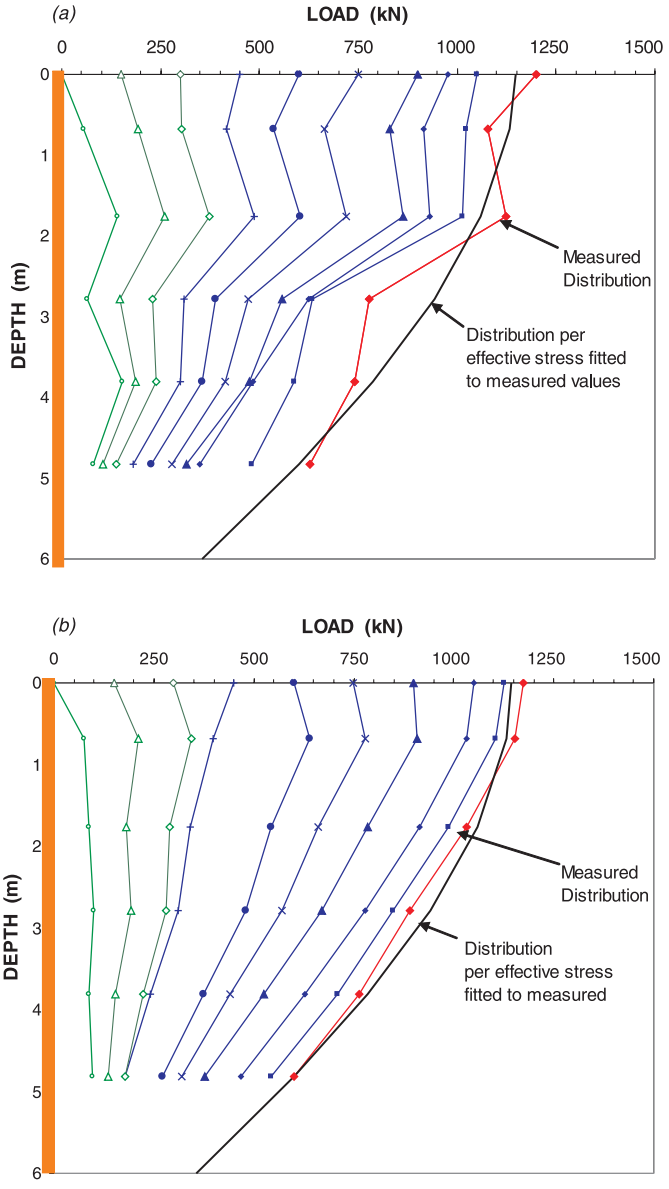

Fig. 21. Load distributions: measured and fitted to effective stress analysis and corrected for residual load. (*a*) Pile E9; (*b*) pile T1.

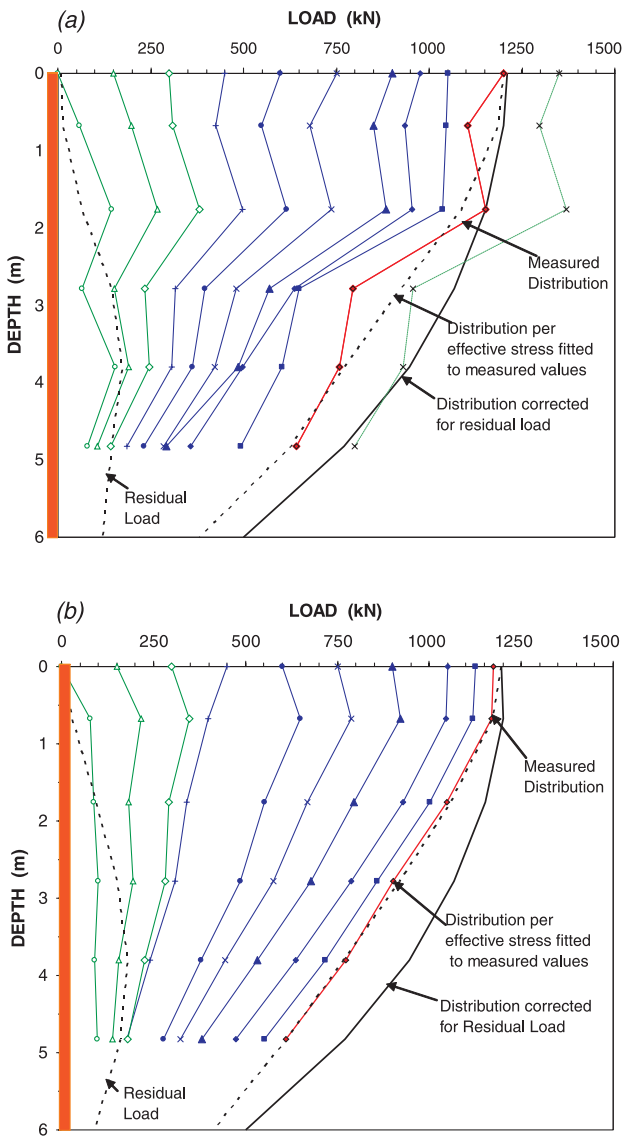

"true" resistance. The actual amount and distribution of residual load cannot be determined for the piles because no assumption of locked-in toe resistance will enable the records to be fitted to a fully mobilized shaft resistance immediately above the pile toe. Therefore, the test piles have not mobilized full positive shaft resistance above the pile toe. However, the *maximum* amount of residual load can be estimated if it is assumed to correspond to fully mobilized shear forces along the entire length of the pile in equilibrium with toe resistance. This maximum results in a total shaft resistance of 360 kN and a toe resistance of 810 kN, which, when fitted to the measured values, correlates to a β coefficient ranging from 0.9 at the bottom of the excavation decreasing to 0.4 at the pile toe and a toe coefficient of 25. These coefficient values are reasonable and in balance with each other. However, fully mobilized negative skin friction along the full length of the pile does not appear to be a reasonable assumption. A compromise assumption is fully mobilized negative skin friction along the upper third of the pile. Below, the residual load is more or less constant or slightly decreasing down to the pile toe. The results of this calculation are shown in Fig. 21, similar to Fig. 20, but the latter figure also includes the estimated residual load and the distribution adjusted for the residual load. The adjusted curves indicate ultimate shaft and toe resistances of 700 and 500 kN for piles E9 and T1. The ultimate resistance values correlate to a constant β coefficient of 1.0 and a toe coefficient of 16. This toe coefficient is still in imbalance with the β coefficient, but the imbalance may be due to disturbance of the soil at the toe from the construction process.

A back-analysis of the loading test on pile C1 using the same β coefficient ($\beta = 0.1$) as evaluated used for the residual load corrected distributions of piles E0 and T1 and adjusting the toe coefficient to fit the capacity to the offset limit load

and the applied maximum load indicates a total shaft resistance of 500 kN and toe resistances of 700 and 1000 kN, respectively. This fitting results in toe coefficients of 50 and 70, respectively, values of which are in balance with the $\beta = 1.0$. Figure 22 shows the calculated load distributions for the test piles. The figures include the distribution calculated using the E–F CPTU method and the CAPWAP-determined distributions for the companion piles.

The measured separation on shaft and toe resistances with residual load adjustment are shown as load-movement curves in Fig. 23 together with the predicted and the CAPWAP-determined curves for piles E9 and T1. Evidently, the unloading and reloading actions have imposed some erratic response in the load-movement curves. The load-movement curves can be reproduced by applying t–z and q–z relations to the mentioned effective stress coefficients for exponents of 0.05 for the shaft and 0.30 for the toe, quite different from the exponents assumed for the author's predicted curves. The pile toe load-movement of pile E9 is shown as calculated from the extrapolation from the strain-gage values and from the cell pressures.

Considering the data quality and the fact that the analysis is made for a companion pile, the CAPWAP-determined total capacity values for the companion piles show good agreement with the test curves (Figs. 15 and 16). With regard to pile C1, this is also true for the movement curve. However, for piles E0 and T1, the CAPWAP-calculated movements differ from the measured load-movement relations. As shown in Fig. 23, this is particularly true for the shaft and toe load-movement curves.

Figure 23 also shows that the shaft and toe predictions submitted by the first author are very much off the mark for piles E9 and T1, particularly with regard to the toe response. It can be claimed that the soil is disturbed at the pile toes and this caused the pile toe response to be reduced. However, this does not make the prediction any better because a good prediction should include the effect of the construction.

Submitted capacity predictions

The 33 submitted predictions of total capacity values for the static loading tests on piles C1, E9, and T1 are presented in the block diagrams in Figs. 24 and 25. For reference to the actual test results, the pile head load-movement curves are superimposed on the diagram. The majority of the submitted predictors underestimated the capacity of the driven pile, while for the bored piles, they overestimated the pile capacities.

The distributions of predicted shaft and toe capacities of the two bored piles are shown in Figs. 26 and 27. The test evaluations show a distinct ultimate shaft resistance response and about half the predictors were reasonably close to these values for piles E9 and T1. The test evaluation showed that no distinct toe resistance was found in the tests. (The predictors were not requested to present a toe capacity defined at a toe movement value.) It is no surprise then that the range of predicted values is very wide.

Conclusions

The results of the five CPT methods show considerable scatter in calculated resistance distributions; total capacity

Fig. 22. Load distributions: static loading tests on piles C1, E9, and T1 at about 100 mm pile-head movement, calculations using the CPTU method, and dynamic tests (CAPWAP) on restrike on piles C2, E0, and T2. (*a*) Pile C1; (*b*) piles E9 and T1.

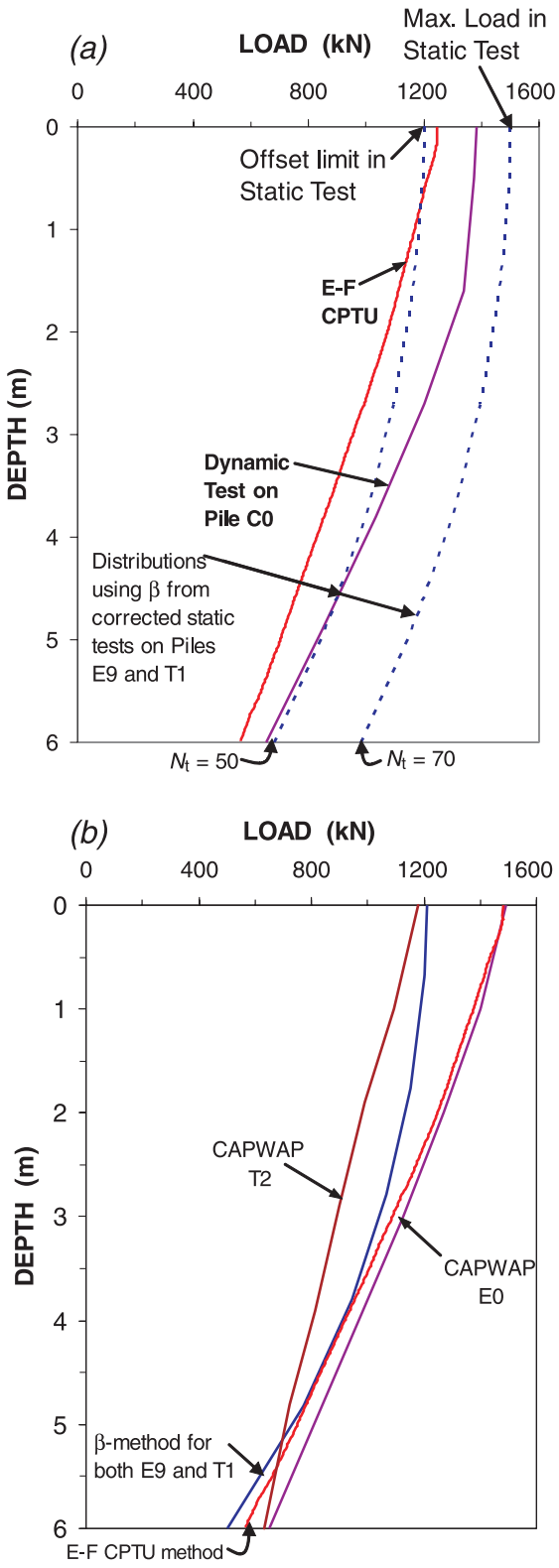

Fig. 23. Load-movement curves for shaft and toe resistance of piles E9 and T1; static loading tests, predicted curves, and dynamic tests (CAPWAP), and values calculated by the E–F CPTU method. (*a*) Pile E9; (*b*) pile T1.

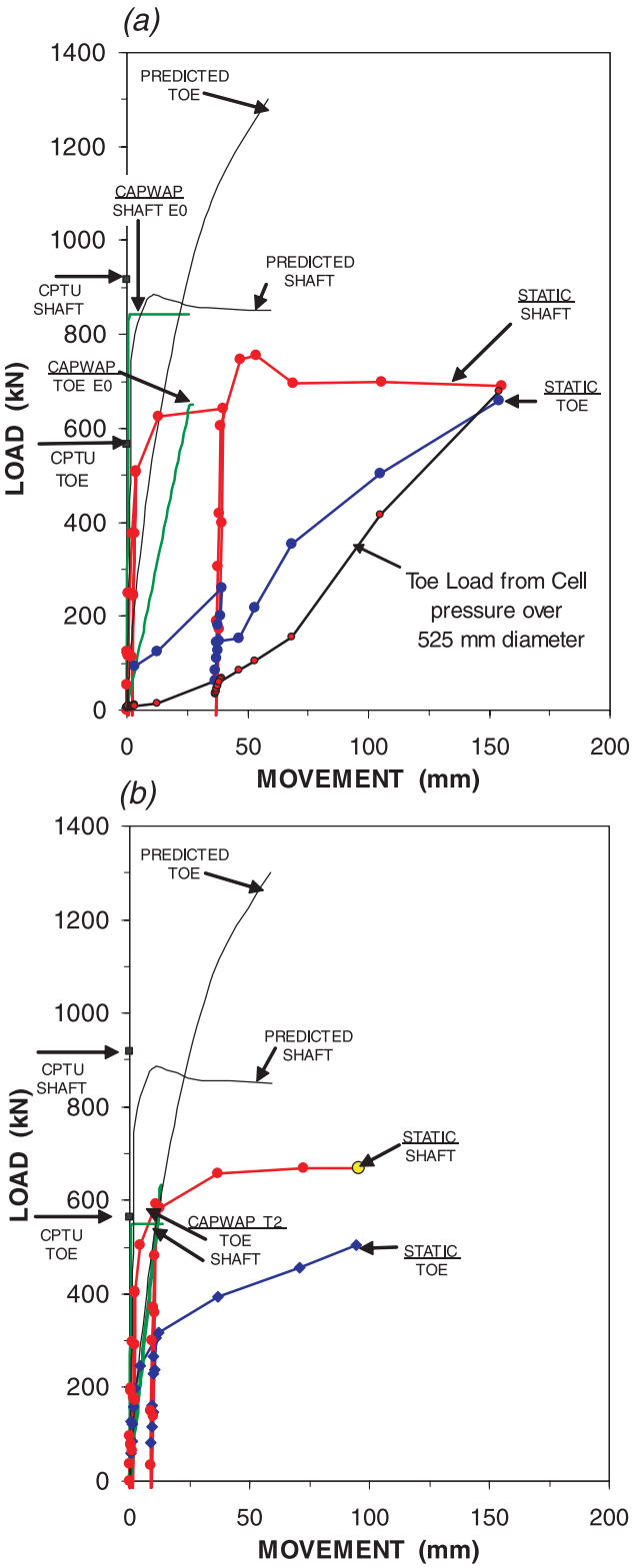

Fig. 24. Total capacities predicted for pile C1.

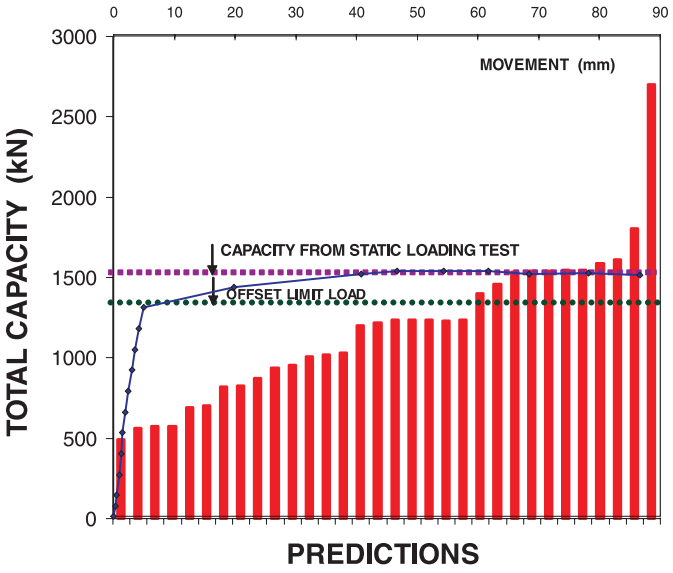

Fig. 25. Total capacities predicted for (*a*) pile E9 and (*b*) pile T1.

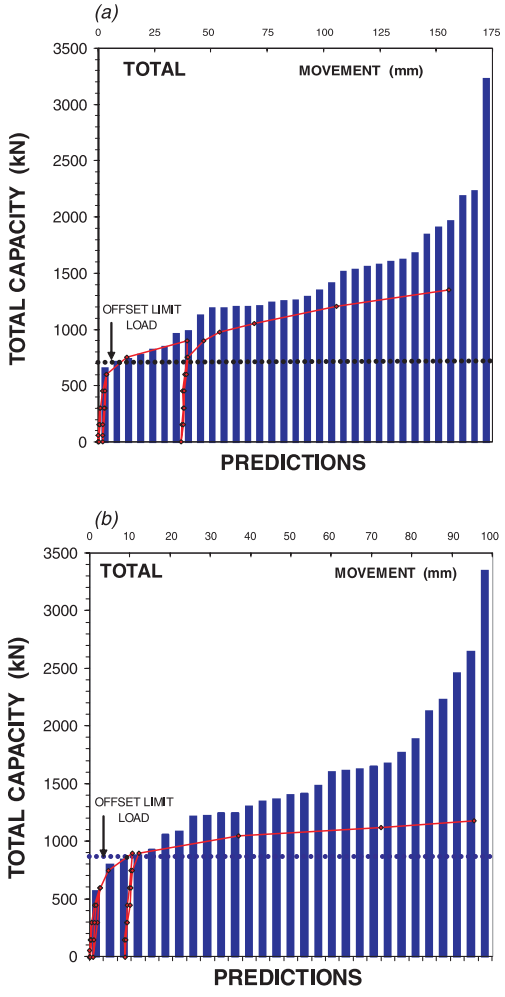

values for the driven and bored piles ranged from 500 to 1400 kN and from 1000 to 1900 kN, respectively. Total shaft resistance for the piles ranged from 100 to 800 kN and from 100 to 1000 kN for the driven and bored piles, respectively. The E–F CPTU method indicated total capacity and shaft resistance values of approximately 1300 and 700 kN

Fig. 26. Shaft capacities predicted for (*a*) pile E9 and (*b*) pile T1.

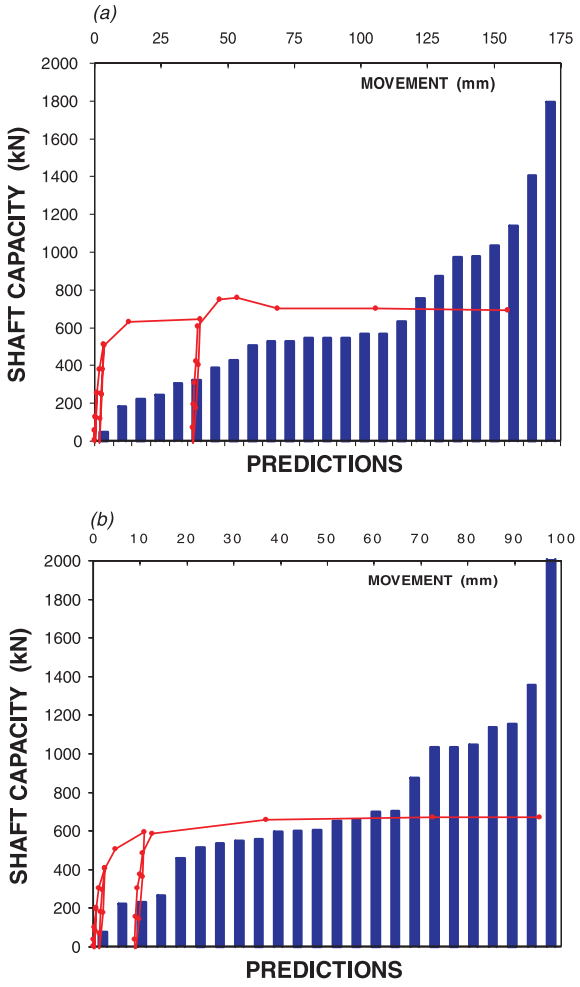

Fig. 27. Shaft capacities predicted for (*a*) pile E9 and (*b*) pile T1.

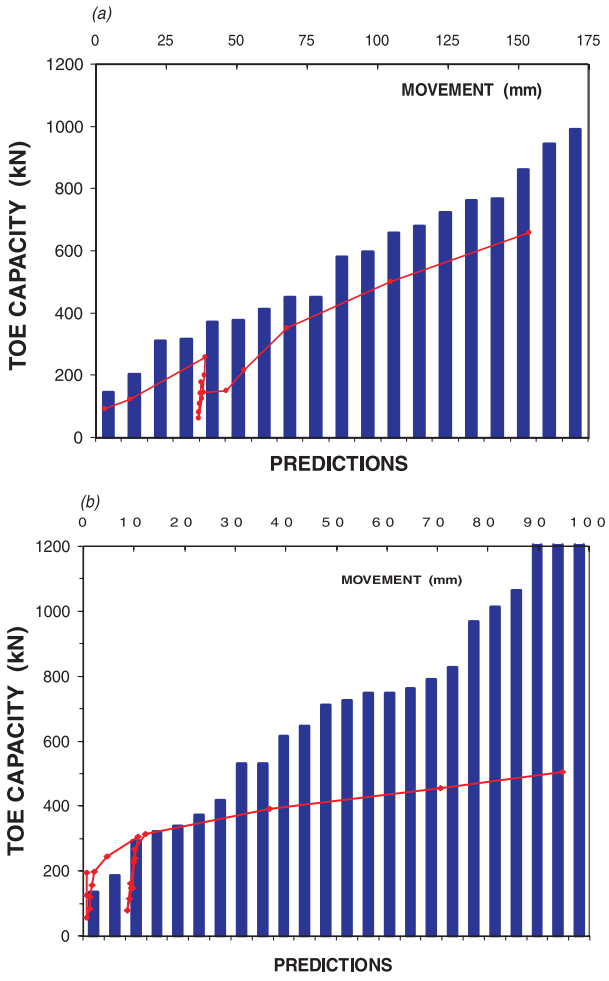

for the driven pile, respectively, and approximately 1500 and 900 kN for the bored piles, respectively.

For effective stress analysis of ultimate pile resistance, published references present very wide ranges of coefficient values. Therefore, where local correlations are lacking, design and prediction calculations require back-calculation of the results from full-scale tests that are representative for the site conditions and geology.

The dynamic restrike records of the companion piles to the test piles are influenced by severe bending of the piles at the gage location, which lowered the quality of the records for analysis. The CAPWAP analyses resulted in a 1400 kN capacity for pile C1 and 1500 and 1450 kN for piles E0 and T2, respectively. The CAPWAP-determined shaft resistances were approximately 730 kN for the driven pile and 850 and 550 kN for piles E0 and T2, respectively. The CAPWAP-determined toe resistances were 650 kN for pile C1 and 620 and 630 kN for piles E0, and T2, respectively.

The static loading tests showed the plunging response capacity of the driven pile to be 1500 kN. However, despite imposed pile movements as large as 100 mm for 1200 kN of applied load, neither of the two bored piles showed signs of having reached an ultimate resistance value. The pile head load-movement responses for the two bored piles are quite similar.

The CAPWAP-calculated capacity for pile C2 is very close to the capacity determined in the static loading test on pile C1. In contrast, neither of the two bored piles showed a distinct capacity value for the static loading tests. The CAPWAP-calculated capacities are close to the maximum load applied. However, the calculated movements are quite different from the measured values and indicate much stiffer response to the applied load than do the static loading tests. It is regrettable that the conditions of reality for the arranging of the prediction event did not allow for restriking of piles C1, E9, and T1 after completion of the static loading tests.

The extensometer measurements in the two bored piles suggest that pile E9 compressed about twice as much as pile T1 for the applied loads, which would mean that the Young's modulus calculated from the nominal shaft diameter would be 20 GPa in pile E9, a low value, and 40 GPa in pile T1, a high value. The reason for the difference in compressibility of the pile is not known, but is probably due to a readout error. Fortunately, evaluation of the measurements of strain does neither require knowledge of the actual diameter nor of the Young's modulus, only of the combination of modulus and cross-sectional area, which is deduced from the strain measurements themselves.

Evaluation of the extensometer measurements for piles E9 and T1 to load distributions indicated apparent values of shaft and toe resistances at the 1200 kN total load for the

100 mm movement of 1000 and 200 kN and 800 and 400 kN, respectively. However, locked-in loads (residual loads) were present in the piles before the static loading test, for which the actual magnitude can only be estimated. A trial-and-error study of the data determined that the presence of residual load caused the direct evaluation of the data to overestimate the shaft resistance by 300 kN and to underestimate the toe resistance by the same amount. Effective stress analysis of the data with an adjustment for these residual loads correlates to a constant β coefficient of 1.0 and a toe coefficient of 16. This toe coefficient is not in balance with the β coefficient, but this may be due to a disturbance of the soil at the toe in the construction process.

A back-analysis of the loading test on pile C1 using the same β coefficient (β = 0.1) used for the residual load corrected distributions of piles E0 and T1 and adjusting the toe coefficient to fit the capacity to the offset limit load and the applied maximum load indicates a total shaft resistance of 700 kN and toe resistances of 700 and 1000 kN, respectively. The fitting results in toe coefficients of 50 and 70, respectively, whose values are in balance with the β coefficient of 1.0.

The compilation of submitted predictions indicates that most predictors underestimated the capacity of the driven pile, while for the bored piles they overestimated the pile capacities. The reason for the overestimation of the capacities of the bored piles is probably due to overestimation of the toe resistances.

Acknowledgements

The authors are grateful to the sponsors: Mota-Engil, SGPS, S.A., Sopecate, S.A., Tecnasol-FGE, S.A., and Teixeira Duarte, S.A. This work was developed under the research activities of Construction Studies Research Centre from FEUP and Institute for Structural Engineering, Territory and Construction from ISTUTL, supported by funding from FCT (Portuguese Science and Technology Foundation). The first author acknowledges the many helpful comments received from Mr. Hicham Salem, AATech Scientific Inc., Ottawa, Canada.

References

Bustamante, M., and Gianeselli, L. 1982. Pile bearing capacity predictions by means of static penetrometer CPT. *In* Proceedings of the Second European Symposium on Penetration Testing, ESOPT II, 24–27 May, Amsterdam. A.A. Balkema, Rotterdam, the Netherlands. Vol. 2, pp. 493–500.

Canadian Geotechnical Society. 1992. Canadian foundation engineering manual (CFEM). 3rd ed. BiTech Publishers, Richmond, B.C.

Costa Esteves, E.F.M. 2005. Testing and analysis of axially loaded piles in a residual soil of granite. M.Sc. thesis, Faculty of Engineering of the University of Porto, Porto, Portugal. [In Portuguese.]

Davisson, M.T. 1972. High capacity piles. *In* Proceedings of Lecture Series on Innovations in Foundation Construction, ASCE, Illinois Section, Chicago, 22 March 1972. American Society of Civil Engineers, New York. pp. 81–112.

DeRuiter, J., and Beringen, F.L. 1979. Pile foundation for large North Sea structures. Marine Geotechnology, **3**(3): 267–314.

European Committee for Standardization. 2004. Eurocode 7: Geotechnical design — General rules. European Committee for Standardization, Brussels. European standard No. EN 1997-1:1994.

Eslami, A. 1996. Bearing capacity of piles from cone penetrometer test data. Ph.D. thesis, University of Ottawa, Ottawa, Ontario.

Eslami, A., and Fellenius, B.H. 1997. Pile capacity by direct CPT and CPTu methods applied to 102 case histories. Canadian Geotechnical Journal, **34**(6): 886–904.

Fellenius, B.H., 1975. Test loading of piles—Methods, interpretation, and proof testing. American Society of Civil Engineers, ASCE Journal of the Geotechnical Engineering Division **101**(GT9): 855–869.

Fellenius B.H. 1989. Tangent modulus of piles determined from strain data. *In* Foundation Engineering: Current Principles and Practices: Proceedings of the 1989 Foundation ASCE, Evaston, Illinois, 25–29 June 1989. *Edited by* F.H. Kulhawy. Geotechnical Special Publication 22. pp. 500–510.

Fellenius, B.H. 1999. Bearing capacity — A delusion? *In* Proceedings of the Deep Foundation Institute 1999 Annual Meeting, Dearborn, Michigan, 14–16 October 1999.

Fellenius, B.H. 2001*a*. Where to plot average loads from telltale measurements in piles. Geotechnical News Magazine, **19**(2): 32–34.

Fellenius, B.H. 2001*b*. From strain measurements to load in an instrumented pile. Geotechnical News Magazine, **19**(1): 35–38.

Fellenius, B.H. 2002*a*. Determining the true distribution of load in piles. *In* Deep Foundations 2002: Proceedings of the International Deep Foundation Congress, Orlando, Florida, 14–16 February 2002. *Edited by* M.W. O'Neill and F.C. Townsend. ASCE Geotechnical Special Publication No. 116. Vol. 2, pp. 1455–1470.

Fellenius, B.H. 2002*b*. Determining the resistance distribution in piles. Part 1: Notes on shift of no-load reading and residual load. Geotechnical News Magazine, **20**(2): 35–38; Determining the resistance distribution in piles. Part 2: Method for determining the residual load. Geotechnical News Magazine, **20**(3): 25–29.

Fellenius, B.H. 2006. Basics of foundation design [online]. Available from http://www.Fellenius.net.

Fellenius, B.H., and Atlaee, A. 1995. The critical depth — How it came into being and why it does not exist. Proceedings of the Institution of Civil Engineers, Geotechnical Engineering, **113**(2): 107–111.

Fellenius B.H., and Goudreault, P.A. 1998. UniPile user manual. Version 4.0. UniSoft Ltd., Calgary, Alberta.

Fellenius, B.H., and Eslami, A. 2000. Soil profile interpreted from CPTu data. *In* Proceedings of Year 2000 Geotechnics Conference, Bangkok, Thailand, 27–30 November 2000. *Edited by* A.S. Balasubramaniam, D.T. Bergado, L. Der Gyey, T.H. Seah, K. Miura, N. Phien wej, and P. Nutalaya. Southeast Asian Geotechnical Society, Asian Institute of Technology, Bangkok, Thailand. Vol. 1, pp. 163–171.

Fellenius, B.H., and Infante, J.-A. 2002. UniCone user manual [online]. Version 1.2. UniSoft Ltd., Calgary, Alberta. Available from http://www.unisoftltd.com/usermanuals/unicone_manual.pdf.

Fellenius, B.H., and Salem, H. 2003. Prediction of response to static loading of three piles at the ISC'2 experimental site. *In* Proceedings of the 2nd International Conference on Site Characterization, Porto, Portugal, 19–22 September 2004. Millpress, Rotterdam, the Netherlands.

Hong Kong Geotechnical Engineering Office (HKGEO). 2005. Foundation design and construction. Draft ed. Government of Hong Kong.

Lambe, T.W. 1973. Predictions in soil engineering. The 13th Rankine Lecture. Géotechnique, **23**(2): 149–202.

Meyerhof, G.G. 1976. Bearing capacity and settlement of pile foundations. The Eleventh Terzaghi Lecture, 5 November 1975. Journal of Geotechnical Engineering, ASCE, **102**(GT3): 195–228.

Robertson, P.K. 1990. Soil classification using the cone penetration test. Canadian Geotechnical Journal, **27**(1): 151–158.

Rollins, K.M., Clayton, R.G., Mikesell, R.C., and Blaise, B.C. 2005. Drilled shaft side friction in gravelly soils. Journal of Geotechnical and Geoenvironmental Engineering, ASCE, **131**(8): 987–1003.

Santos, J.A., and Viana da Fonseca, A. 2003. Installation parameters for the international prediction event on the behavior of bored, CFA, and driven piles in ISC'2 experimental site [on line]. Available from http://www.fe.up.pt/isc-2/.

Santos, J.A., Duarte, R.J.L, Viana da Fonseca, A., and daCosta Esteves, E.F.M. 2005. ISC'2 experimental site — Prediction and performance of instrumented axially loaded piles. *In* Proceedings of the 16th International Conference of Soil Mechanics and Geotechnical Engineering, Osaka, 21–25 September 2005. Millpress, Rotterdam, the Netherlands. Vol. 2, pp. 2171–2174.

Schmertmann, J.H. 1978. Guidelines for cone test, performance, and design. Federal Highway Administration, Washington, D.C. Report FHWA-TS-78209.

Tumay, M.T., and Fakhroo, M. 1981. Pile capacity in soft clays using electric QCPT data. *In* Proceedings of a Conference on Cone Penetration Testing and Experience, St. Louis, Missouri, 26–30 October 1981. American Society of Civil Engineers, New York. pp. 434–455.

Viana da Fonseca, A. 2003. Characterizing and deriving engineering properties of a saprolitic soil from granite in Porto. *In* Characterization and Engineering Properties of Natural Soils: Proceedings of the International Workshop, Singapore, 2–4 December 2002. *Edited by* T.S. Tan, K.K. Phoon, D.W. Hight, and S. Leroueil. Swets & Zeitlinger, Lisse, the Netherlands. Vol. 2, pp. 1341–1378.

Viana da Fonseca, A., Carvalho, J., Ferreira, C., Tuna, C., Costa, E., and Santos, J. 2004. Geotechnical characterization of a residual soil profile: the ISC'2 experimental site. *In* Geotechnical and Geophysical Site Characterization. *Edited by* A. Viana da Fonseca and P.W. Mayne. Millpress, Rotterdam, the Netherlands. Vol. 2, pp. 1361–1369.

Viana da Fonseca, A., Carvalho, J., Ferreira, C., Santos, J.A., Almeida, F., Pereira, E., Feliciano, J., Grade, J., and Oliveira, A. 2006. Characterization of a profile of residual soil from granite combining geological, geophysical, and mechanical testing techniques. Geotechnical and Geological Engineering, **24**: 1307–1348.